



HAL
open science

Comprehensive analysis of alternative downscaled soil moisture products

Sabah Sabaghy, Jeffrey P. Walker, Luigi J. Renzullo, Ruzbeh Akbar, Steven Chan, Julian Chaubell, Narendra Das, R. Scott Dunbar, Dara Entekhabi, Anouk Gevaert, et al.

► **To cite this version:**

Sabah Sabaghy, Jeffrey P. Walker, Luigi J. Renzullo, Ruzbeh Akbar, Steven Chan, et al.. Comprehensive analysis of alternative downscaled soil moisture products. *Remote Sensing of Environment*, 2020, 239, pp.111586. 10.1016/j.rse.2019.111586 . hal-03035074

HAL Id: hal-03035074

<https://hal.science/hal-03035074>

Submitted on 2 Dec 2020

HAL is a multi-disciplinary open access archive for the deposit and dissemination of scientific research documents, whether they are published or not. The documents may come from teaching and research institutions in France or abroad, or from public or private research centers.

L'archive ouverte pluridisciplinaire **HAL**, est destinée au dépôt et à la diffusion de documents scientifiques de niveau recherche, publiés ou non, émanant des établissements d'enseignement et de recherche français ou étrangers, des laboratoires publics ou privés.

Comprehensive analysis of alternative downscaled soil moisture products

Sabah Sabaghy ^{*1}, Jeffrey P. Walker¹, Luigi J. Renzullo², Ruzbeh Akbar⁵, Steven Chan³, Julian Chaubell³, Narendra Das³, R. Scott Dunbar³, Dara Entekhabi⁵, Anouk Gevaert⁴, Thomas J. Jackson⁶, Alexander Loew¹¹, Olivier Merlin⁷, Mahta Moghaddam⁸, Jian Peng^{11,12,13}, Jinzheng Peng^{9,10}, Jeffrey Piepmeier⁹, Christoph Rüdiger¹, Vivien Stefan⁷, Xiaoling Wu¹, Nan Ye¹, and Simon Yueh³

¹Department of Civil Engineering, Monash University, VIC 3800, Australia.

²Fenner School of Environment and Society, The Australian National University, Canberra, Australia.

³Jet Propulsion Laboratory, California Institute of Technology, Pasadena, CA 91109 USA.

⁴Earth and Climate Cluster, Department of Earth Sciences, VU Amsterdam, Amsterdam, The Netherlands.

⁵Department of Civil and Environmental Engineering, Massachusetts Institute of Technology, Cambridge, MA 02139 USA.

⁶U.S. Department of Agriculture ARS, Hydrology and Remote Sensing Laboratory, Beltsville, MD 20705 USA.

⁷Centre d'Etudes Spatiales de la Biosphère (CESBIO), 18 Avenue, Edouard Belin, bpi 2801, Toulouse 31401, France.

⁸Department of Electrical Engineering, University of Southern California, Los Angeles, CA 90089 USA.

⁹Goddard Space Flight Center, 8800 Greenbelt Rd, Greenbelt, MD 20771, USA.

¹⁰Universities Space Research Association, Columbia, MD, USA.

¹¹Department of Geography, University of Munich (LMU), 80333 Munich, Germany.

¹²School of Geography and the Environment, University of Oxford, OX1 3QY Oxford, UK.

¹³Max Planck Institute for Meteorology, 20146 Hamburg, Germany.

Journal: Remote Sensing of Environment

This is a PDF file of the pre-print version of the manuscript that has been published in the Journal Remote Sensing of Environment.

Please cite this article as: Sabah Sabaghy, Jeffrey P. Walker, Luigi J. Renzullo, Ruzbeh Akbar, Steven Chan, Julian Chaubell, Narendra Das, R. Scott Dunbar, Dara Entekhabi, Anouk Gevaert, Thomas J. Jackson, Alexander Loew, Olivier Merlin, Mahta Moghaddam, Jian Peng, Jinzheng Peng, Jeffrey Piepmeier, Christoph Rüdiger, Vivien Stefan, Xiaoling Wu, Nan Ye, Simon Yueh, Comprehensive analysis of alternative downscaled soil moisture products, Remote Sensing of Environment, Volume 239, 2020, 111586, ISSN 0034-4257.

<https://doi.org/10.1016/j.rse.2019.111586>.

<http://www.sciencedirect.com/science/article/pii/S0034425719306066>

1 **Abstract**

2 Recent advances in L-band passive microwave remote sensing provide an unprecedented opportunity
3 to monitor soil moisture at ~ 40 km spatial resolution around the globe. Nevertheless, retrieval of the
4 accurate high spatial resolution soil moisture maps that are required to satisfy hydro-meteorological and
5 agricultural applications remains a challenge. Currently, a variety of downscaling, otherwise known as
6 disaggregation, techniques have been proposed as the solution to disaggregate the coarse passive mi-
7 crowave soil moisture into high-to-medium resolutions. These techniques take advantage of the strengths
8 of both the passive microwave observations of soil moisture having low spatial resolution and the spatially
9 detailed information on land surface features that either influence or represent soil moisture variability.
10 However, such techniques have typically been developed and tested individually under differing weather
11 and climate conditions, meaning that there is no clear guidance on which technique performs the best.
12 Consequently, this paper presents a quantitative assessment of the existing radar-, optical-, radiometer-,
13 and oversampling-based downscaling techniques using a singular extensive data set collected specifically
14 for that purpose, being the Soil Moisture Active Passive Experiment (SMAPEX)-4 and -5 airborne field
15 campaigns, and the OzNet *in situ* stations, to determine the relative strengths and weaknesses of their
16 performances. The oversampling-based soil moisture product best captured the temporal and spatial
17 variability of the reference soil moisture overall, though the radar-based products had a better temporal
18 agreement with airborne soil moisture during the short SMAPEX-4 period. Moreover, the difference
19 between temporal analysis of products against *in situ* and airborne soil moisture reference data sets
20 pointed to the fact that relying on *in situ* measurements alone is not appropriate for validation of
21 spatially enhanced soil moisture maps.

22 **Keywords:** Downscaling, Disaggregation, Inter-comparison, High resolution, Soil moisture, SMAP,
23 SMOS, SMAPEX

24 **1 Introduction**

25 Soil moisture influences land-atmosphere interaction via fluxes of energy and water, and thus
26 impacts weather and climate conditions (Seneviratne et al., 2010), hydrology (Corradini, 2014;
27 Koster et al., 2004, 2010) and agricultural production (Bolten et al., 2010). The ability to pro-
28 vide reliable, spatially distributed and temporally consistent measurements of soil moisture will
29 therefore be of great benefit. Key to providing such information economically across the globe
30 has been the development of L-band passive microwave remote sensing technology (Entekhabi
31 et al., 2010; Kerr et al., 2016). The passive L-band microwave approach is widely accepted as
32 the optimum technology for soil moisture estimation (Entekhabi et al., 2010).

33 There are currently two L-band passive microwave satellite missions dedicated to monitoring
34 the near surface soil moisture every 2 to 3 days: i) the European Space Agency (ESA) Soil
35 Moisture and Ocean Salinity (SMOS), launched in November 2009 as the first ever dedicated
36 satellite for soil moisture mapping, and ii) the National Aeronautics and Space Administration
37 (NASA) Soil Moisture Active Passive (SMAP), launched in January 2015 as the first ever
38 satellite to combine a radar and radiometer to produce an enhanced resolution soil moisture
39 product. Together, the SMOS and SMAP missions have provided a continuity of dedicated
40 satellite soil moisture observations globally since 2010 (Kerr et al., 2016).

41 Soil moisture estimates at the native resolution of both the SMOS and SMAP radiome-
42 ters are at a coarse scale of approximately 40 km (but provided on 25 km and 36 km grid
43 spacing, respectively), which is not sufficient to meet the spatial resolution requirements of
44 hydro-meteorological, agricultural and carbon cycle applications (e.g. Entekhabi et al., 2010;
45 Molero et al., 2016). However, the inclusion of an L-band radar on SMAP was to provide spatial
46 scale improvement of the radiometric observations by combining with the L-band radiometer
47 observations (Entekhabi et al., 2010; O'Neill et al., 2010). The sensitivity of radar backscatter
48 to soil moisture dynamics and the geophysical properties of the soil surface was expected to

49 contribute to improvement of the retrievals' accuracy and disaggregation of radiometric soil
50 moisture estimates (Chauhan, 1997; Petropoulos et al., 2015). However, loss of coincident radar
51 imaging in July 2015, due to a hardware anomaly, meant that an alternative downscaling ap-
52 proach had to be sought. Moreover, there is no radar sensor aboard SMOS. Consequently,
53 alternative downscaling techniques have been applied to the two soil moisture missions, with
54 the aim to accurately and efficiently increase the resolution of SMOS and SMAP passive L-band
55 soil moisture (and/or brightness temperature).

56 Reviews of techniques for downscaling passive microwave data for high resolution soil mois-
57 ture mapping have been recently published by Sabaghy et al. (2018) and Peng et al. (2017).
58 Downscaling methods exploit both the accuracy of the passive L-band microwave observations
59 and the high resolution spatial variability of the ancillary data. Accordingly, downscaling tech-
60 niques include, but are not limited to radar-, optical-, radiometer-, and oversampling-based
61 methods.

62 The radar-based downscaling techniques (Akbar and Moghaddam, 2015; Bindlish et al.,
63 2008; Das et al., 2011, 2014; Piles et al., 2009; Zhan et al., 2006) are based on radar-radiometer
64 combination algorithms which enhance the spatial detail of coarse radiometric soil moisture
65 using the spatially varied information on land surface features provided by radar. The extent of
66 correlation between backscatter and soil moisture, and sensitivity of backscatter to soil moisture
67 changes determine the success of radar-based downscaling techniques in estimating the variation
68 of soil moisture in space (Wu et al., 2014).

69 The basic concept behind the optical-based downscaling techniques (e.g. Fang et al., 2013;
70 Merlin et al., 2006, 2008a,b, 2012, 2013; Piles et al., 2011, 2012, 2013) is the feature space
71 between vegetation index and surface temperature in the shape of a triangle/trapezoid (e.g.
72 Carlson et al., 1994; Gillies and Carlson, 1995) which indicates wet and dry conditions at its
73 edges. This feature space adjusts the sensitivity of land surface temperature to soil moisture as
74 a function of vegetation cover density and canopy type.

75 The radiometer-based downscaling technique (e.g. Gevaert et al., 2015; Santi, 2010) uses
76 radiometric emissions at higher frequency (Ka-band, 26 to 40 GHz) to provide information
77 about spatial variability of the surface when there is no rainfall event (Gevaert et al., 2015).
78 The advantage of the radiometer- (over the optical-) based approach lies in the capacity of
79 radiometer imagery to deliver ancillary data under all-weather conditions and being less affected
80 by the soil surface condition. However, the radiometer-based technique is not able to improve
81 the resolution of soil moisture content to the same extent as the optical-based techniques due
82 to the coarser resolution of that data, as the resolution of downscaled products is dictated by
83 that of the ancillary data used for the downscaling.

84 The oversampling-based method (Chan et al., 2018; Chaubell, 2016) applies an interpolation
85 technique which rescales the brightness temperature values to 30 km and posted onto a 9 km
86 grid. Consequently, it creates the most optimal brightness temperature by aggregating bright-
87 ness temperature values that are centred near a particular radius with a relatively short length of
88 intervals. For the methods that downscale the brightness temperature (e.g. oversampling- and
89 radiometer-based techniques), soil moisture retrieval is then conducted on the higher resolution
90 brightness temperature using the same passive microwave soil moisture retrieval algorithm as
91 for the coarse observations.

92 A diversity of downscaling approaches exist, typically developed and tested under differing
93 weather and climate conditions. However, until now there has been no rigorous test to as-
94 sess which downscaling methodology yields the best overall soil moisture estimation at higher
95 resolution over a specific location and climate condition, which can only be achieved by com-
96 paring the approaches on a common data set. Therefore, this paper presents a comprehensive
97 inter-comparison of the various downscaling techniques against each other and reference data
98 to determine the relative strengths and weaknesses of their performance. This is the first
99 comprehensive assessment of the complete range of different radar-, optical-, radiometer-, and
100 oversampling-based downscaled soil moisture products which are readily available using the

101 same set of evaluation data, in order to take a step towards multi-sensor high resolution soil
102 moisture retrieval for typical Australian landscapes. The performance of downscaled products
103 was also benchmarked against the radiometer-only retrievals of SMAP and SMOS.

104 This paper has focused on analysing the performance of downscaled soil moisture products
105 for a typical Australian landscape and climate. However, deep insight into the performance of
106 downscaled soil moisture products requires similar inter-comparisons be undertaken for different
107 climate conditions and landscapes around the world. Consequently, the curators of such data
108 sets (eg. Soil Moisture Active Passive Validation EXperiment (SMAPVEX)) are encouraged to
109 conduct similar soil moisture inter-comparisons over their sites.

110 **2 Study area and reference data sets**

111 The Yanco agricultural area in New South Wales, Australia, was chosen to conduct this research.
112 Yanco has a landscape and climate that is representative of much of southeast Australia. The
113 climate is classified as semi-arid based on the Köppen-Geiger climate classification system. An
114 average annual amount of about 400 mm precipitation falls in the Yanco area throughout the
115 year, and its' minimum and maximum average annual temperature is equal to 11°C and 24°C,
116 respectively (Bureau of Meterology, 2018). The Yanco area is located on a flat plain in the
117 Murrumbidgee River catchment and contains a network of soil moisture and rainfall monitoring
118 stations as part of OzNet (Smith et al., 2012). The locations of OzNet stations installed in the
119 Yanco region are shown as black dots in Figure 1. Moreover, the soil moisture measurements
120 utilized for evaluation in this study are those over the 0-5 cm depth of soil, which is widely
121 accepted as being the monitoring depth of L-band passive microwave soil moisture and their
122 downscaled soil moisture products. These data are available from <http://www.oznet.org.au>.
123 The temporal pattern of soil moisture is consistent with the occurrence of precipitation events
124 with wetting and drying cycles for the 1st April to 1st November 2015 study period as shown in
125 Figure 2. The study area is relatively flat, with a variety of land use, soil and vegetation types,

126 thus making Yanco an appropriate site for evaluation of downscaling algorithm performance.

127 Over the Yanco region, the Soil Moisture Active Passive Experiment (SMAPEX)-4 and -5
128 airborne campaigns were designed to cover an area of about 71 km \times 89 km (145.98° - 146.75°E
129 longitude and 34.22° - 35.03°S latitude, see Figure 1) for the purpose of calibration and validation
130 of SMAP soil moisture products. These experiments were carried out during the Australian
131 autumn (SMAPEX-4, from the 1st to 22nd May 2015 when crops were in the early growth stage
132 or under cultivation) and spring (SMAPEX-5, from 7th to 27th September 2015 when crops
133 were in the maturity stage). During SMAPEX-4 and -5 airborne field campaigns, airborne L-
134 band passive microwave brightness temperature were collected using the Polarimetric L-band
135 Multi-beam Radiometer (PLMR) instrument concurrent with the SMAP and SMOS satellite
136 overpasses. The PLMR radiometer, having similar characteristics to that of the SMAP and
137 SMOS missions, provided brightness temperature at both vertical and horizontal polarization
138 with 1 km resolution, and thus soil moisture for an equivalent depth to that from SMAP
139 and SMOS. It collected dual-polarized brightness temperature measurements with six-beams at
140 across-track incidence angles of $\pm 7^\circ$, $\pm 21.5^\circ$, and $\pm 38.5^\circ$, which were then angle normalized to
141 $\pm 38.5^\circ$ using the approach of Ye et al. (2015) before retrieval of the soil moisture. These airborne
142 observations were supported by ground sampling activities that were conducted concurrent to
143 flight acquisitions, to provide information about vegetation (biomass, vegetation water content,
144 leaf area index, etc.) and surface roughness, which were used for the soil moisture retrieval.
145 The Hydraprobe Data Acquisition System (HDAS) - a dielectric probe - was also used to
146 measure top 5 cm intensive *in situ* soil moisture data at 250 m grid spacing coincident with
147 airborne sampling. The intensive HDAS soil moisture measurements were collected to evaluate
148 the performance of airborne PLMR soil moisture retrievals.

149 The PLMR radiometric brightness temperature observations were used to derive a reference
150 airborne soil moisture data set. This retrieval process included application of the L-band Mi-
151 crowave Emission of the Biosphere (L-MEB, Wigneron et al., 2007) radiative transfer model

152 to PLMR brightness temperature (Ye et al., in review). The vegetation water content used
153 by the L-MEB model for soil moisture retrieval was estimated using the relationships devel-
154 oped by Gao et al. (2015), which convert the derived Normalized Difference Vegetation Index
155 (NDVI, Rouse et al., 1974) from daily 250 m MODerate resolution Imaging Spectroradiome-
156 ter (MODIS) reflectance products (MOD09GQ) to vegetation water content. Utilized surface
157 roughness and vegetation parameters were obtained from Panciera et al. (2008, 2009) and in-
158 formation about land surface types were collected from the studies conducted by Grant et al.
159 (2008) and Wigneron et al. (2007). In order to estimate effective soil temperature, the average
160 of soil temperature measurements at 2.5 and 40 cm depth were calculated using measurements
161 from the six temporary monitoring stations over the Yanco area.

162 In order to quantify the accuracy of the reference airborne PLMR soil moisture maps and
163 their propagation into the evaluation statistics for the downscaled soil moisture, the airborne
164 PLMR soil moisture retrievals were compared against the HDAS measurements over all intense
165 soil moisture sampling areas for SMAPEX-4 and -5 airborne field campaigns (Figure 3). The
166 intensive HDAS soil moisture measurements were averaged to 3 km for the comparison with
167 the airborne PLMR soil moisture aggregated to 3 km. While overall evaluation of 3 km PLMR
168 soil moisture pixels are reported in Figure 3, the accuracy assessment was also conducted for
169 each dominant land surface type with similar results. An overall RMSD of $0.04 \text{ m}^3 \text{ m}^{-3}$ and
170 R^2 of 0.76 was achieved for 3 km SMAPEX-4 and -5 soil moisture data, showing that airborne
171 soil moisture could be used as a suitable reference for evaluation of downscaled soil moisture
172 products. The PLMR soil moisture maps at 1 km were not evaluated in a similar way as there
173 were only a few HDAS intense soil moisture measurements (≤ 4) available within each 1 km
174 footprint, yielding the analysis unreliable. In addition, the HDAS measurements within the 1
175 km scale had a large variability due to the range of moisture condition.

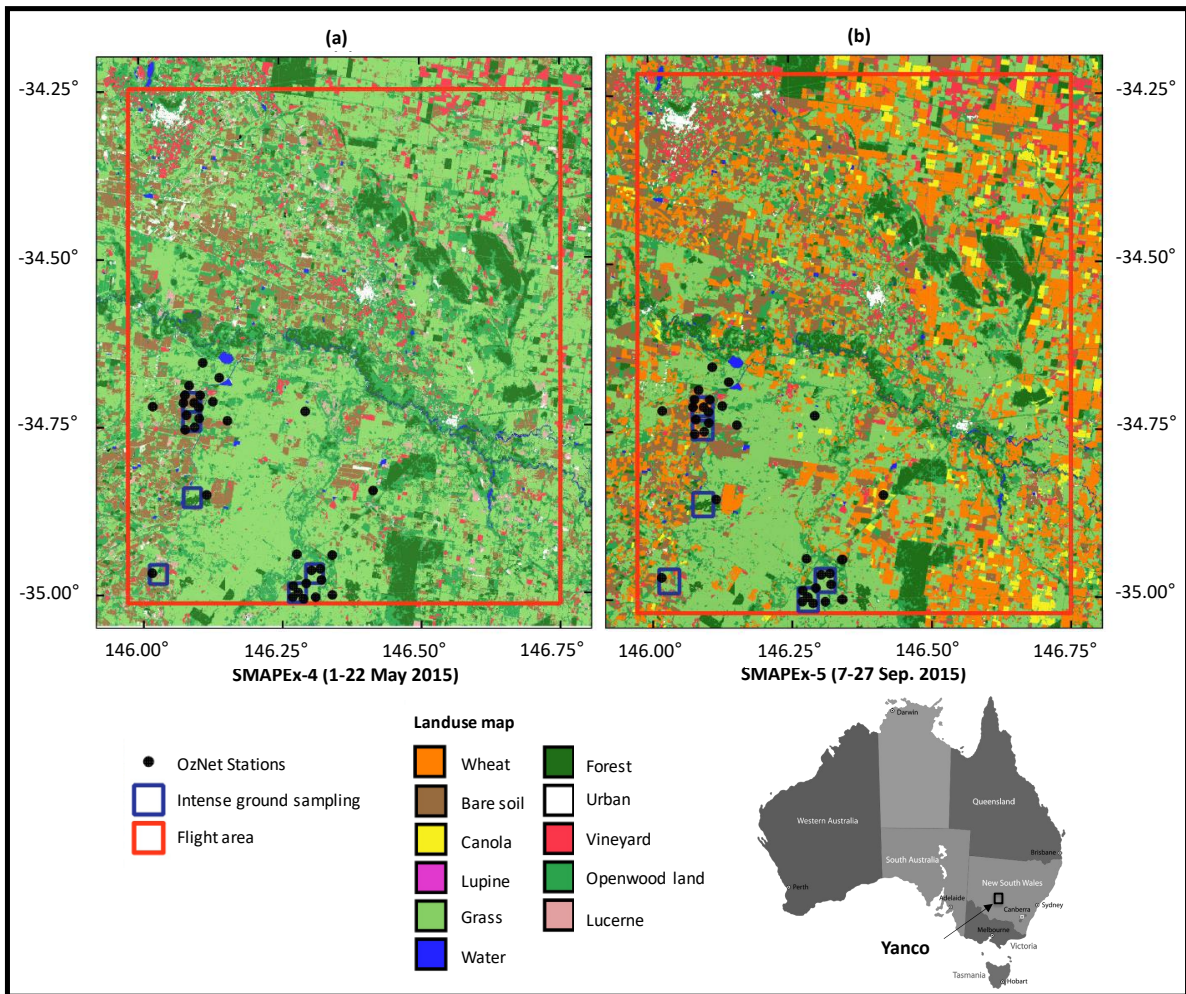


Figure 1: The study area for (a) SMAPEX-4 and (b) SMAPEX-5 airborne field campaigns conducted in the Yanco region in south east of Australia along with red rectangles which delineate the coverage of airborne measurements of each campaign, being 71 km × 85 km for SMAPEX-4 and 71 km × 89 km for SMAPEX-5. Blue rectangles show the locations of the intense ground samplings and black dots are the OzNet *in situ* monitoring stations. Note: the landuse maps were created using two Landsat-8 Operational Land Imager (OLI) images at 30 m spatial resolution, acquired on the 10th of June and 30th of September 2015, to match the dates of the SMAPEX-4 and -5 airborne field campaigns.

176 3 Downscaling Methods

177 This study comprehensively evaluated the performance of soil moisture downscaled products
 178 against each other in terms of accuracy and capability to capture the variability of soil moisture
 179 in space and time. The products were derived from a variety of current downscaling techniques,
 180 categorized as either radar-, optical-, radiometer-and oversampling-based techniques. The soil
 181 moisture products evaluated in this study are listed in Table 1 along with the downscaling
 182 techniques and approaches, product definitions, key references, and main downscaling inputs as

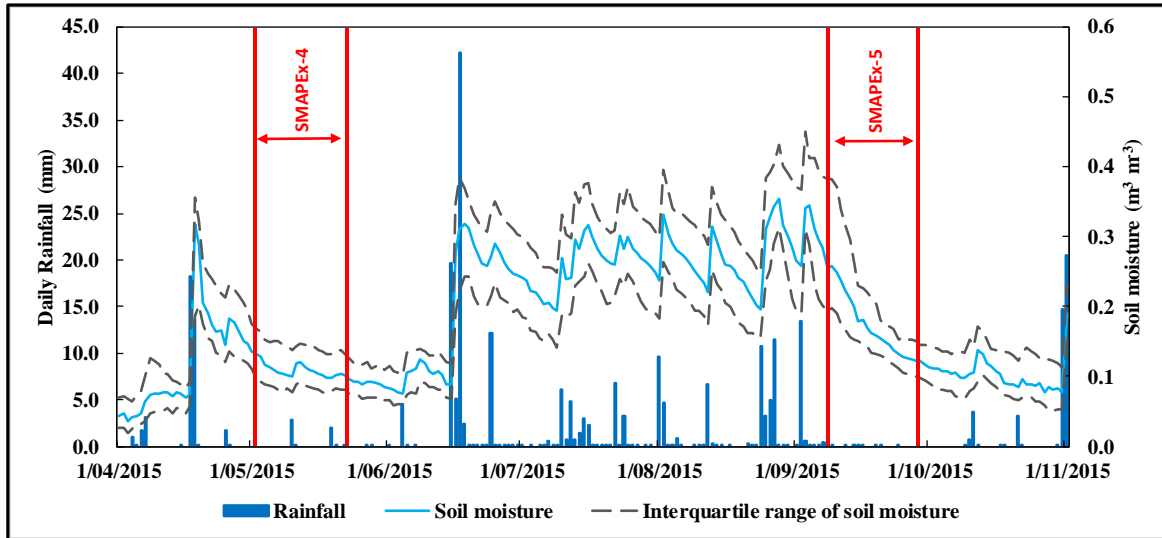


Figure 2: Time series of the OzNet top 5 cm *in situ* soil moisture and rainfall measurements for the period between 1st April and 1st November 2015 used in this study. The solid light blue line and dashed gray lines show the median and interquartile range of soil moisture measurements, respectively. The dark blue bars show the mean daily rainfall over the Yanco region.

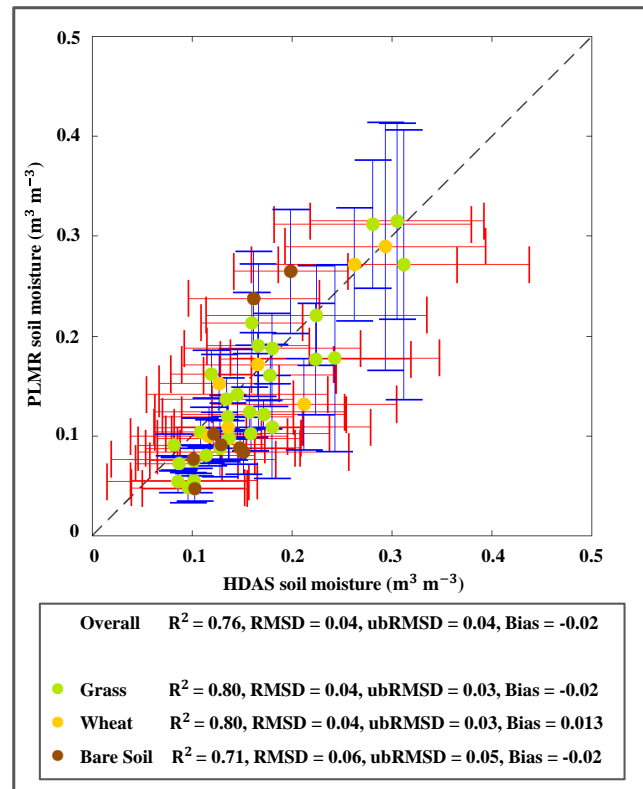


Figure 3: Comparison of SMAPEX-4 and -5 PLMR soil moisture estimates at 3 km against aggregated intense HDAS soil moisture measurements to 3 km. Whiskers in red show the standard deviation of aggregated HDAS measurements to 3 km, while whiskers in blue show the standard deviation of aggregated PLMR soil moisture estimates to 3 km.

183 applicable. The downscaling techniques were benchmarked against the SMOS and SMAP coarse
184 passive microwave observations to provide insight about the impact of downscaling approaches
185 on the accuracy of soil moisture retrievals, and inter-compared over the Yanco region using the
186 airborne soil moisture maps collected during the SMAPEX-4 and -5 airborne field campaigns,
187 as well as OzNet *in situ* measurements for the period between 1 April and 1 November 2015.
188 The intention of this comparison was to reveal if downscaled soil moisture products surpass
189 the coarse passive soil moisture estimates in terms of accuracy, and to quantitate the extent of
190 possible improvement (or deterioration). In this study, the SMAP Level 3 Radiometer Global
191 Daily soil moisture (version 3) posted on the 36 km EASE-Grid, and the daily global SMOS
192 Level 3 radiometric soil moisture retrievals, obtained from the 43 km mean spatial scale SMOS
193 observations posted on the 25 km grid (SMOS operational MIR CLF31A/D version 3.00 ob-
194 tained from the CATDS website: <https://www.catds.fr/Products/Products-access>), were
195 evaluated for this purpose.

196 **Radar-based techniques**

197 The SMAP soil moisture was downscaled from 36 to 9 km using the radar-based downscaling
198 techniques, including: i) the baseline active/passive method of SMAP (Das et al., 2014) and,
199 ii) the Multi-Objective Evolutionary Algorithm (MOEA) by Akbar et al. (2016). The baseline
200 active/passive combination technique is the main procedure used by the SMAP science team
201 to produce the SMAP Radar/Radiometer soil moisture products at 9 km resolution prior to
202 the radar failure. This downscaling algorithm was developed to take advantage of the strengths
203 of passive and active microwave observations, being accurate and high resolution soil moisture
204 mapping, respectively. The baseline algorithm disaggregated the SMAP radiometric brightness
205 temperature through combination with SMAP radar backscatter. This procedure, which inher-
206 ited background knowledge from the work of Piles et al. (2009) and Das et al. (2011), includes:
207 i) calibrating model parameters from a linear regression analysis of the time series of brightness

Table 1: Summary table on the soil moisture downscaling products used in the inter-comparison according to the downscaling techniques and approaches. Included is the product definition, key references, and main downscaling inputs as applicable.

Spatial Resolution	Downscaling Technique	Downscaling Approach	Product Definition	Product name	Key Reference	Main Downscaling Inputs	
1 km	Optical-based	Disaggregation based on Physical And Theoretical scale Change (DisPATCH)	Ascending DisPATCH	SMOS DisPATCHA	Merlin et al. (2013)	* SMOS Level 3 radiometric soil moisture retrievals on 25 km grid posting	
			SMOS			* Daily MODIS land surface temperature	
			Descending DisPATCH			* Digital Elevation Model (DEM) outputs	
			product with Descending SMOS	SMOS DisPATCHD		* 16 day composite MODIS vegetation index products	
9 km	Oversampling-based	Backus-Gilbert interpolation method	VTICI-based downscaled	SMAP VTICI	Peng et al. (2015, 2016)	* SMAP Level 3 Radiometer Global Daily soil moisture on 36 km grid posting	
			product with Descending SMAP			* 4 day composite MODIS Leaf Area Index at 1 km	
			VTICI-based downscaled			* Daily Aqua MODIS day and night time land surface temperature	
			product with Descending SMOS	SMOS VTICI		* SMOS Level 3 radiometric soil moisture retrievals on 25 km grid posting	
			Ascending Enhanced			* 4 day composite MODIS Leaf Area Index at 1 km	
			product with Ascending SMAP	SMAP EnhancedA	Chaubell et al. (2016)	* Daily Aqua MODIS day and night time land surface temperature	
			SMAP			* Ascending SMAP L1B Radiometer Half-Orbit Time-Ordered Temperatures at 47 km \times 36 km	

Table 1 (continued)

Spatial Resolution	Downscaling Technique	Downscaling Approach	Product Definition	Product name	Key Reference	Main Downscaling Inputs
9 km	Oversampling-based	Backus-Gilbert interpolation method	Descending Enhanced product with Descending SMAP	SMAP EnhancedD	Chaubell et al. (2016)	* Descending SMAP L1B Radiometer Half-Orbit Time-Ordered Brightness Temperatures at 47 km × 36 km
			The SMAP active/passive baseline algorithm	Active/Passive product with SMAP	SMAP A/P	Das et al. (2014)
9 km	Radar-based	Multi-Objective Evolutionary Algorithm (MOEA)	MOEA product with SMAP	SMAP MOEA	Akbar et al. (2016)	* SMAP radar backscatter at 3 km
			Smoothing Filter-based Intensity Modulation (SFIM)	SFIM-based product with SMAP	SMAP SFIM	Gevaert et al. (2015)
10 km	Radiometer-based	Smoothing Filter-based Intensity Modulation (SFIM)	Ascending Passive SMOS	SMOS PassiveA	Jacquette et al. (2013), ATBD	N/A
			Descending Passive SMOS	SMOS PassiveD	O,Neill et al. (2018), ATBD	N/A
25 km	N/A	N/A	Ascending Passive SMAP	SMAP PassiveA		
			Descending Passive SMAP	SMAP PassiveD		
36 km	N/A	N/A	Ascending Passive SMAP	SMAP PassiveA		
			Descending Passive SMAP	SMAP PassiveD		

208 temperature-radar backscatter pairs at radiometric footprint (36 km), and ii) combination of the
209 coarse resolution brightness temperature and medium resolution radar backscatter (9 km) using
210 a linear function, which utilizes the calibrated slope from the predecessor step. Soil moisture
211 is then estimated by applying the radiative transfer model (single channel algorithm, Jackson,
212 1993) to the downscaled brightness temperature. These estimates are available at the NASA
213 National Snow and Ice Data Center Distributed Active Archive Center (NSIDC DAAC) website
214 as SMAP Level 3 Radar/Radiometer Global Daily 9 km EASE-Grid Soil Moisture, Version 3
215 (SPL3SMAP, access link: <https://nsidc.org/data/SPL3SMAP/versions/3>).

216 The MOEA is a physical-based downscaling technique (Akbar et al., 2016), which implicitly
217 disaggregates the radiometric soil moisture from the coarse scale of 36 km to the medium scale
218 of 9 km using a multi-objective optimization approach. This technique is based on the combi-
219 nation of optimized radar- and radiometer-only soil moisture estimations and is developed to
220 compromise on the performance of the forward electromagnetic emission and scattering models.
221 The MOEA technique finds an optimum solution by including evaluation of multiple objective
222 functions within each iteration. Based on stochastic operators, the MOEA procedure gives more
223 weight to the most accurate soil moisture retrievals from either radar backscatter or brightness
224 temperature. The MOEA technique was applied to the SMAP L2 Radiometer Half-Orbit 36
225 km EASE-Grid Soil Moisture, Version 2 and SMAP L1C Radar Half-Orbit High-Resolution σ^0
226 Data on 1 km Swath Grid, Version 1 (SPL1CS0) pairs.

227 **Optical-based Techniques**

228 Two types of physically based optical downscaling techniques were applied to the daily global
229 SMOS Level 3 radiometric soil moisture retrievals, obtained from the 43 km mean spatial scale
230 SMOS observations posted on the 25 km grid (SMOS operational MIR CLF31A/D, version 3.00
231 obtained from the Centre Aval de Traitement des Données SMOS (CATDS) website) and SMAP
232 Level 3 Radiometer Global Daily soil moisture posted on the 36 km EASE-Grid. Disaggregation

233 was based on the Physical And Theoretical scale Change (DisPATCh; Merlin et al., 2013) and
234 the Vegetation Temperature Condition Index (VTCI; Peng et al., 2015, 2016) approaches to
235 achieve a 1 km spatial resolution.

236 The DisPATCh uses the Soil Evaporative Efficiency (SEE, i.e. ratio of actual to poten-
237 tial soil evaporation) derived from the daily MODIS land surface temperature (MOD11A1 and
238 MYD11A1 products) and a 16 day composite MODIS vegetation index product (MOD13A2)
239 at 1 km resolution, as the main soil moisture downscaling component. MODIS land surface
240 temperature is decoupled in its soil and vegetation components based on a partitioning method
241 (Moran et al., 1994) with the decoupled surface temperature corrected for the impact of ele-
242 vation using an ancillary 1 km resolution Digital Elevation Model (DEM) according to Merlin
243 et al. (2013). The SEE proxy is an appropriate downscaling index because: i) it has a relatively
244 constant daily characterization for non-cloudy skies (Crago and Brutsaert, 1996) and ii) it cor-
245 responds well with soil moisture changes (Anderson et al., 2007). The DisPATCh technique was
246 applied to the SMOS ascending and descending soil moisture observations resulting in two Dis-
247 PATCh products, the morning/ascending DisPATCh (DisPATChA) and afternoon/descending
248 DisPATCh (DisPATChD).

249 The VTCI technique uses the high resolution VTCI as the downscaling factor. The VTCI
250 is a thermal based proxy which is used as a drought monitoring index (Wang et al., 2001). It is
251 calculated based on the triangular/trapezoidal feature space constructed from 4 day composite
252 MODIS Leaf Area Index (LAI, MCD15A3) at 1 km resolution and the daily Aqua MODIS day-
253 and night-time land surface temperature difference ($\Delta LST_{\text{day-night}}$, MYD11A1).

254 **Radiometer-based techniques**

255 Downscaled SMAP soil moisture retrievals were also produced at 10 km using the radiometer-
256 based Smoothing Filter-based Intensity Modulation (SFIM) model used by Gevaert et al. (2015).
257 The SFIM methodology is based on the multi-sensor image fusion technique designed by (Liu,

258 2000). Success of this technique in producing downscaled Landsat Thematic Mapper data to
259 a higher spatial resolution using the high resolution Satellite Pour l’Observation de la Terre
260 images, motivated Santi (2010) to employ this technique for the purpose of soil moisture down-
261 scaling. In the SFIM procedure a weighting factor is used to downscale the 36 km SMAP Level
262 2 brightness temperature (SPL2SMP) to 10 km. The downscaling factor used here is the ra-
263 tio between the Advanced Microwave Scanning Radiometer-Earth Observing System (AMSR2)
264 Ka-band brightness temperature for each grid cell at 10 km and the average of Ka-band bright-
265 ness temperature across the coarse scale of the SMAP brightness temperature observations.
266 From downscaled SMAP brightness temperature, soil moisture content was estimated through
267 application of the Land Parameter Retrieval Model (LPRM, Owe et al., 2001, 2008).

268 **Oversampling-based techniques**

269 An oversampling-based technique (Chan et al., 2018; Chaubell, 2016), based on the Backus-
270 Gilbert interpolation method (Backus and Gilbert, 1970, 1967), was also used to enhance
271 not only the spatial scale of SMAP brightness temperature but also its accuracy. Soil mois-
272 ture was then derived by applying a radiative transfer model to the brightness temperature
273 posted onto a 9 km grid. This technique was applied to the morning/descending (D) and af-
274 ternoon/ascending (A) SMAP level 1B Radiometer Half-Orbit Time-Ordered brightness Tem-
275 perature products at $47 \text{ km} \times 36 \text{ km}$, resulting in two series of products: the EnhancedD and
276 EnhancedA, respectively. Free access to the SMAP enhanced soil moisture products is granted
277 (https://nsidc.org/data/SPL3SMP_E/versions/2). The Backus-Gilbert is an optimal inter-
278 polation theory that provides the closest observation to what perhaps would be measured by the
279 radiometric instrument at the interpolation point (Poe, 1990). To this aim, all the brightness
280 temperature values that are centred near a particular radius within a relatively short length of
281 intervals are aggregated to a spatial resolution higher than the resolution and/or footprint of
282 observations. The extent of improvement of the spatial resolution is determined by the sampling

283 density and the overlap in the response functions of the instrument at measurement locations.
284 Long and Daum (1998) found out that when the sampling pattern is denser there is a better
285 opportunity for the spatial resolution enhancement of observations. The non-uniformity of over-
286 lapping measurement is another factor which facilitates better resolution enhancement (Long,
287 2003).

288 **4 Evaluation methodology**

289 This section describes the evaluation procedure that is summarised in Figure 4. Here down-
290 scaled products are evaluated against a comprehensive reference data set that includes the
291 OzNet *in situ* soil moisture measurements and SMAPEX-4 and -5 airborne PLMR soil mois-
292 ture maps. The coarse passive SMAP and SMOS soil moisture products were also compared
293 against the same reference data set providing a baseline scenario. Unlike previous studies (e.g.
294 Al-Yaari et al., 2019; Chen et al., 2018) which assessed the accuracy of SMAP and SMOS pas-
295 sive microwave soil moisture products at their coarse scale (posted onto 36 and 25 km spatial
296 resolution, respectively), this study only assessed the accuracy of the coarse resolution products
297 in the context of being a reference for assessing the skill of the downscaled products relative to
298 the uniform field assumption. Accordingly, this assessment was to understand to what extent
299 the downscaling techniques improved the spatial soil moisture estimates over the simplistic as-
300 sumption that the soil moisture is a uniform field over coarse resolution pixels. This evaluation
301 is meant to serve as a quantitative assessment of the improvement in the downscaled products
302 over the coarse soil moisture products, applied directly at the same spatial resolution as the
303 comparable downscaled product. Consequently, prior to the evaluation of coarse SMAP and
304 SMOS soil moisture products, each product was mapped onto a 1 and 9 km grid, with the value
305 of each coarse pixel assigned to each higher resolution pixel lying within the original pixel.

306 The evaluation against OzNet measurements was conducted over the period between 1st
307 April and 1st November 2015, while the time frame of the evaluation against airborne PLMR

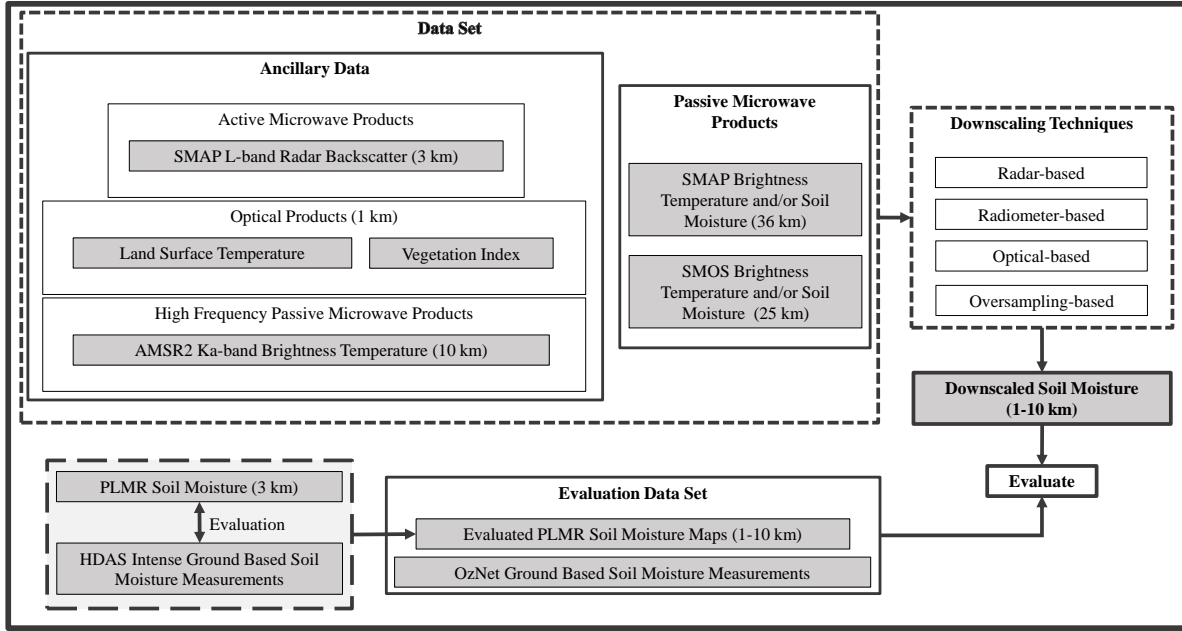


Figure 4: Schematic of the procedure used for evaluation of the downscaled soil moisture retrievals against airborne PLMR and OzNet *in situ* soil moisture measurements.

308 soil moisture was associated with the temporal extent of the SMAPEX-4 and -5 airborne field
 309 campaigns. The evaluation included a temporal analysis of downscaled products against both
 310 the OzNet and airborne PLMR soil moisture. In the temporal analysis, time series of soil mois-
 311 ture values from each pixel of modelled estimates were compared against corresponding values
 312 from the reference PLMR maps and/or aggregated OzNet measurements to the products pixel
 313 scale. Moreover, the spatial analysis was carried out against the airborne PLMR soil mois-
 314 ture. In the spatial analysis, daily maps of estimates were compared against the corresponding
 315 reference map. From the temporal and spatial match-ups mentioned above, the performance
 316 metrics were calculated, including bias, coefficient of determination (R^2), Root Mean Square
 317 Deviation (RMSD), unbiased RMSD (ubRMSD), and slope of the linear regression. In order to
 318 provide readers with more information about the performance of soil moisture products, rela-
 319 tive accuracy of the soil moisture products was calculated and reported in the Appendix. The
 320 relative accuracy parameters were calculated by dividing Bias, RMSD, and ubRMSD values by
 321 the average of reference soil moisture content values through time and space for temporal and
 322 spatial analysis, respectively.

323 The optical-based downscaled products were evaluated at two different scales: i) 1 km being
324 the original scale of the optical-based products, and ii) 9 km being the scale of radar- and
325 oversampling-based retrievals. For the evaluation at 9 km, the optical-based products herein
326 DisPATCh and VTCI were upscaled to the SMAP A/P scale of 9 km, using the arithmetic
327 average. The evaluation at 9 km was conducted to make the comparison system consistent
328 across downscaled soil moisture products being mainly available at 9 km.

329 **4.1 Evaluation against OzNet in situ soil moisture measurements**

330 To compare downscaled products against OzNet, soil moisture measurements from individual
331 stations were averaged within the grid cell of each product. However, for the 1 km grid, any
332 pixel with a coincident OzNet station was considered for comparison. Therefore, 28 and 30
333 pixels at the 1 km scale of the DisPATCh and VTCI products, respectively, were compared
334 against the corresponding OzNet stations. For the grid scales larger than 1 km, comparisons
335 were made across the pixels that had a large number of OzNet stations (more than or equal to
336 four) within their scale. Figure 5 shows the selected pixels at the medium scales of 9 and 10
337 km at which downscaled soil moisture products were evaluated.

338 **4.2 Evaluation against SMAPEX-4 and -5 PLMR soil moisture maps**

339 The evaluation of downscaled products against PLMR required pairing of the PLMR soil mois-
340 ture maps with the nearest available downscaled products to the PLMR flights, when coincident
341 downscaled data were not available. The nearest available products were selected based on infor-
342 mation about the rainfall occurrence over the study area and minimal average absolute change
343 ($\leq 0.02 \text{ m}^3 \text{ m}^{-3}$) of OzNet soil moisture measurements between the flight dates and those of
344 the nearest available products in time. The date of the nearest available observations to PLMR
345 flights is written on soil moisture thumbnail plots (Figure 6 and 7 provided in the results section)
346 when data were not coincident. To resolve scale mismatches between soil moisture products

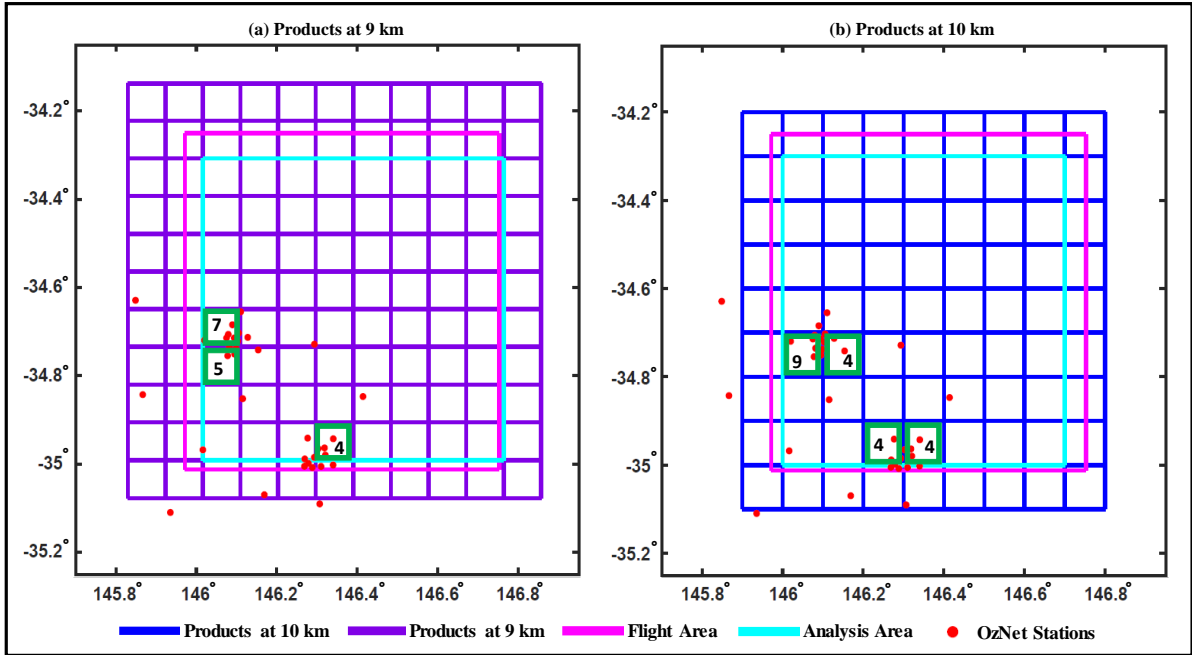


Figure 5: Schematic of the downscaled soil moisture product grids at (a) 9 km and (b) 10 km. The SMAPEX-4 and -5 flight coverage and location of OzNet stations are highlighted in magenta rectangles and red dots, respectively. The cyan rectangle shows the common analysis area for both airborne field campaigns. Green squares show the chosen pixels for analysis of soil moisture products against OzNet measurements. These pixels contain the largest number of OzNet stations (more than four); the number of available stations is written in the pixel.

347 and PLMR soil moisture maps, the original PLMR soil moisture footprints were first processed
 348 onto the same 1 km grid, and then averaged within the grid cell of each 9 or 10 km resolution
 349 product.

350 The main comparison scenario of downscaled products against airborne PLMR soil mois-
 351 ture was developed to discard the seasonal performance of downscaled products because the
 352 operational application of downscaled soil moisture products should be regardless of climate
 353 conditions (Sabaghy et al., 2018). The analysis herein used the entire downscaled soil moisture
 354 data captured during both the SMAPEX-4 and -5 airborne field campaigns. Moreover, the sea-
 355 sonal performance of downscaled soil moisture products was examined for the Austral autumn
 356 (March-May, using SMAPEX-4 data) and spring (September-November using SMAPEX-5 data)
 357 as a complementary scenario, in order to understand the seasonal performance and uncertainties
 358 of the soil moisture products.

359 Radar-based soil moisture products were only available for the period between 15 April and

360 7 July 2015 when the SMAP radar was still transmitting data. Thus, radar-based products
361 were evaluated only for the SMAPEX-4 airborne field campaign. The seasonal evaluation of the
362 performance of other downscaled products was conducted when enough (4 or more) coincident
363 downscaled soil moisture maps were available. Accordingly, the performance analysis of the
364 VTCI-based products was not possible for the SMAPEX-4 period as only one SMOS VTCI and
365 two SMAP VTCI soil moisture maps were captured due to cloud.

366 In order to address the potential variation in number of different downscaled products avail-
367 able for comparison, and eliminate the impact on evaluation, only downscaled products collected
368 on 3, 6, 11, 20 and 22 May 2015 during SMAPEX-4 were evaluated herein. This evaluation
369 was undertaken for the SMAPEX-4 period only because the radar-, optical-, radiometer-and
370 oversampling-based products were all available over this period.

371 **5 Results**

372 Time series of downscaled and observed airborne PLMR soil moisture maps during the SMAPEX-
373 4 and -5 airborne field campaigns are shown in Figure 6 and Figure 7, respectively. These figures
374 show the performance of the downscaled products in capturing the spatio-temporal variability
375 of soil moisture. The airborne PLMR soil moisture estimates at 1 km have consistency with the
376 occurrence of precipitation events, mimicking the dry down cycle observed during SMAPEX-5
377 and the rainfall interrupted drying spell during the SMAPEX-4 (Figure 2). There is no clear
378 evidence from Figures 6 and 7 to show that any downscaling process is clearly superior to an-
379 other for disaggregation of SMAP and/or SMOS, but among the downscaled products available
380 over the SMAPEX-4 period, DisPATCH and VTCI products - especially at 9 km - revealed the
381 best visual agreement with the spatial and temporal pattern of airborne PLMR soil moisture
382 compared to other products. However, a limitation of the optical approach is that it cannot
383 deliver any soil moisture downscaling under cloudy skies because of the lack of cloud-free optical
384 imagery, which is the key component or input in the optical downscaling process. This short-

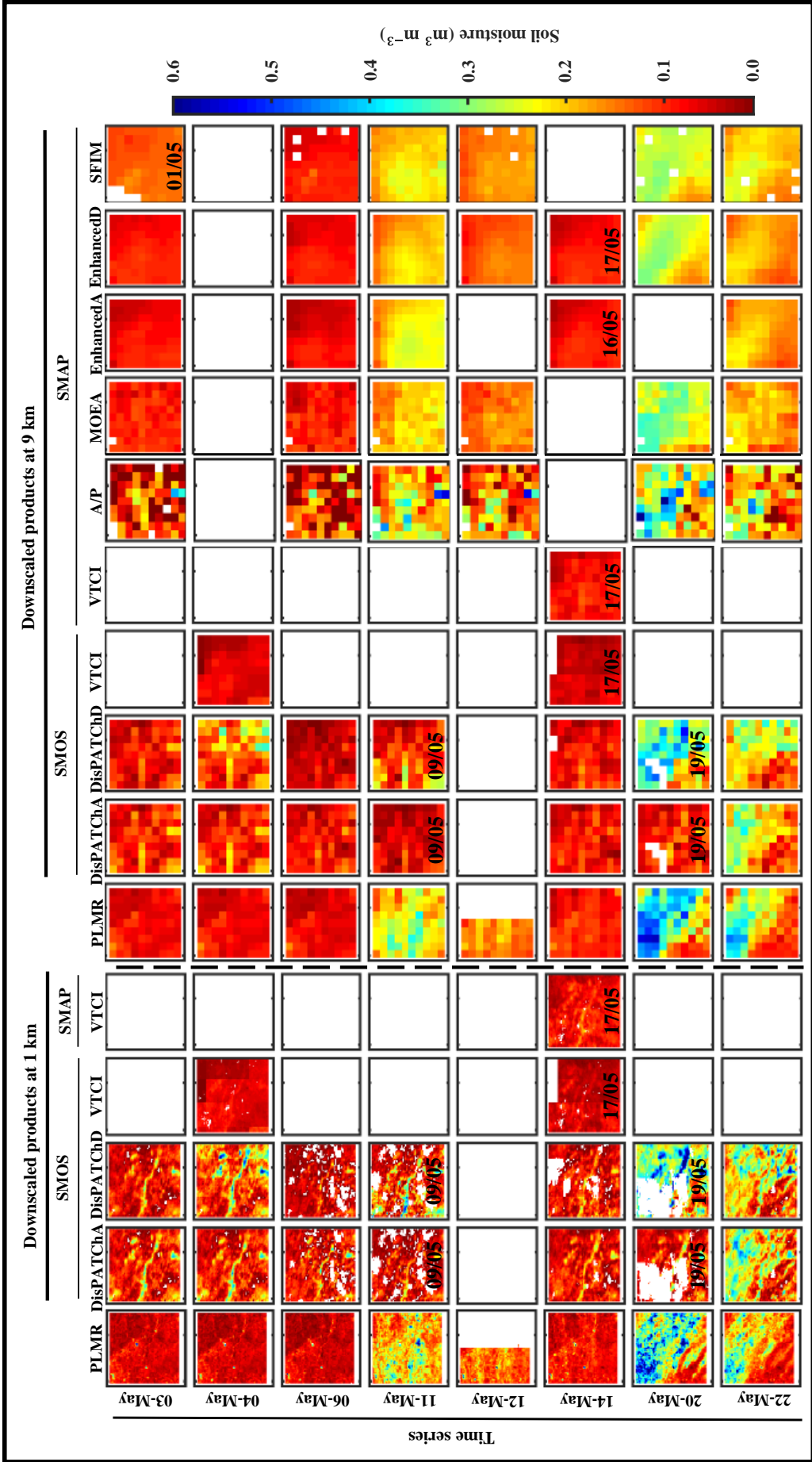


Figure 6: Time series plots of PLMR observed reference soil moisture estimates and the range of downscaled soil moisture estimates for the Yanco region during the SMAPEX-4 period. DisPATCH, VTICI-based and PLMR soil moisture maps are presented at their original scale of 1 km as well as 9 km after aggregation. The date is written on soil moisture plots for the nearest available observations to PLMR flight days when coincident overpass data are not available. Note: missing data are shown in white colour.

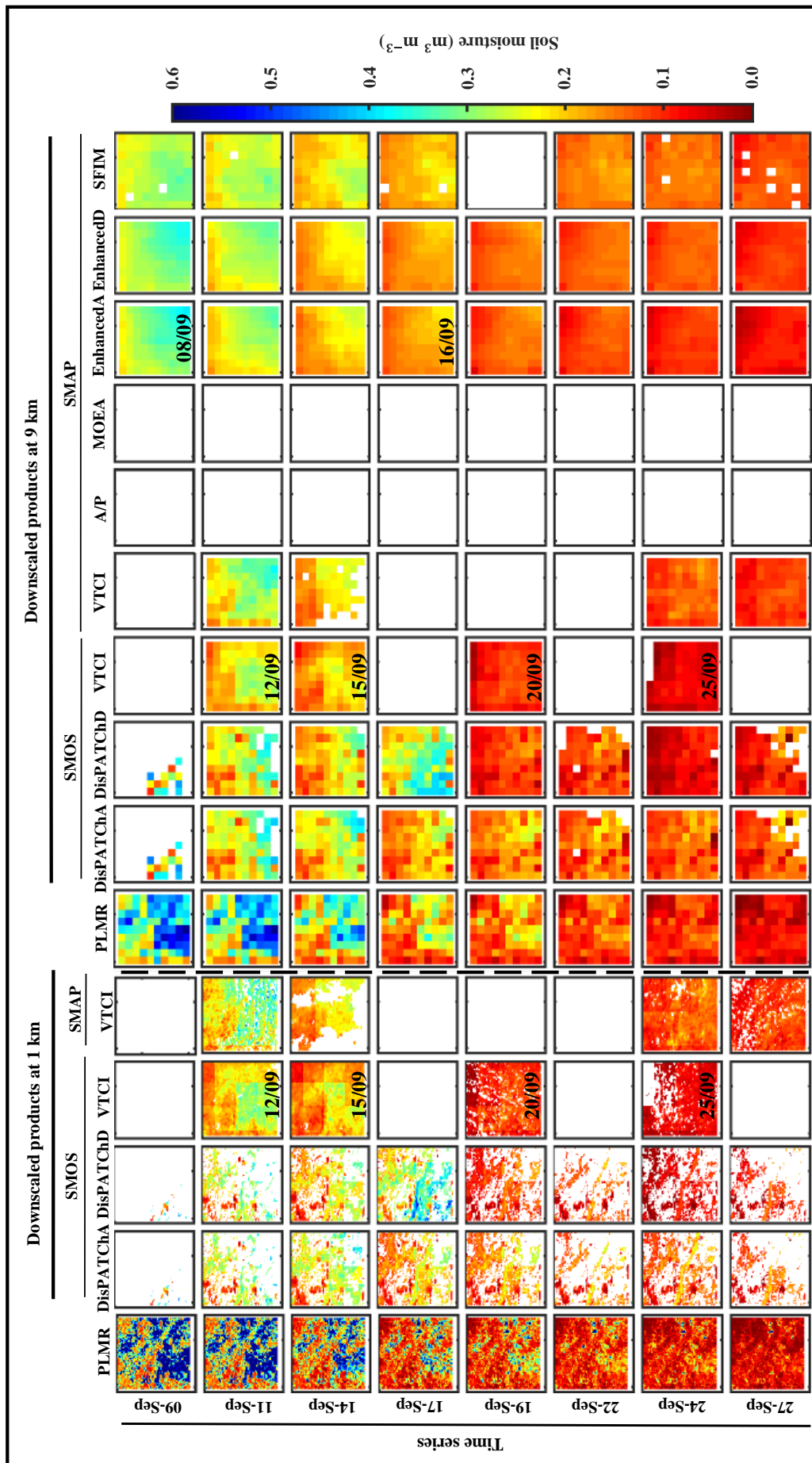


Figure 7: As for Figure 6 but for the SMAPEX-5 period.

385 coming of optical imagery resulted in the reduced availability of the VTCI-based downscaled
386 soil moisture, which uses the difference of day and night land surface temperature in derivation
387 of its downscaling index. The lack of access to optical observations, which is more pronounced
388 for the SMAPEX-5 period, is unlike microwave-based approaches where there are no such gaps
389 in data. The microwave-techniques are in general capable of soil moisture downscaling under
390 all-weather conditions. This capability is due to microwave observations being able to pass
391 through non-raining clouds unaffected. The success of DisPATCH and VTCI products in cap-
392 turing the soil moisture spatio-temporal variability is followed by the radar-based downscaled
393 product, namely the SMAP MOEA, which was only available for the SMAPEX-4 period.

394 The temporal evolution of downscaled soil moisture products at 9 km was also compared
395 with that of aggregated OzNet measurements to 9 km (Figure 8) showing a significant level of
396 agreement between them. The majority of downscaled soil moisture values do not match the
397 median OzNet soil moisture closely, but are in the range of aggregated OzNet measurements.
398 However, there are also a few days on which downscaled soil moisture estimates laid outside
399 the OzNet measurement range. Erratic oscillations were observed for the SMOS PassiveD soil
400 moisture estimates between July to September 2015. These oscillations are reportedly due to
401 a poor constraint on the Vegetation Optical Depth (VOD) during the retrieval process. This
402 is specific to the level 3 algorithm used in this analysis (SMOS operational MIR CLF31A/D
403 product, version 3.00) and does not occur with the level 2 algorithm. Accordingly, a new level
404 3 retrieval algorithm has recently been developed by the SMOS science team to constrain VOD
405 during 3-orbit periods and is currently being validated. The accuracy of downscaled soil mois-
406 ture products is known to be affected by the accuracy of the coarse passive soil moisture from
407 which downscaled products are derived (Peng et al., 2017; Sabaghy et al., 2018). Accordingly,
408 the soil moisture values larger than $0.55 \text{ m}^3 \text{ m}^{-3}$ were excluded from the statistical analysis.
409 However, the SMOS DisPATCHD and SMOS VTCI downscaled soil moisture estimates were
410 shown to rarely reach values larger than $0.5 \text{ m}^3 \text{ m}^{-3}$ in mid August, similar to SMOS PassiveD

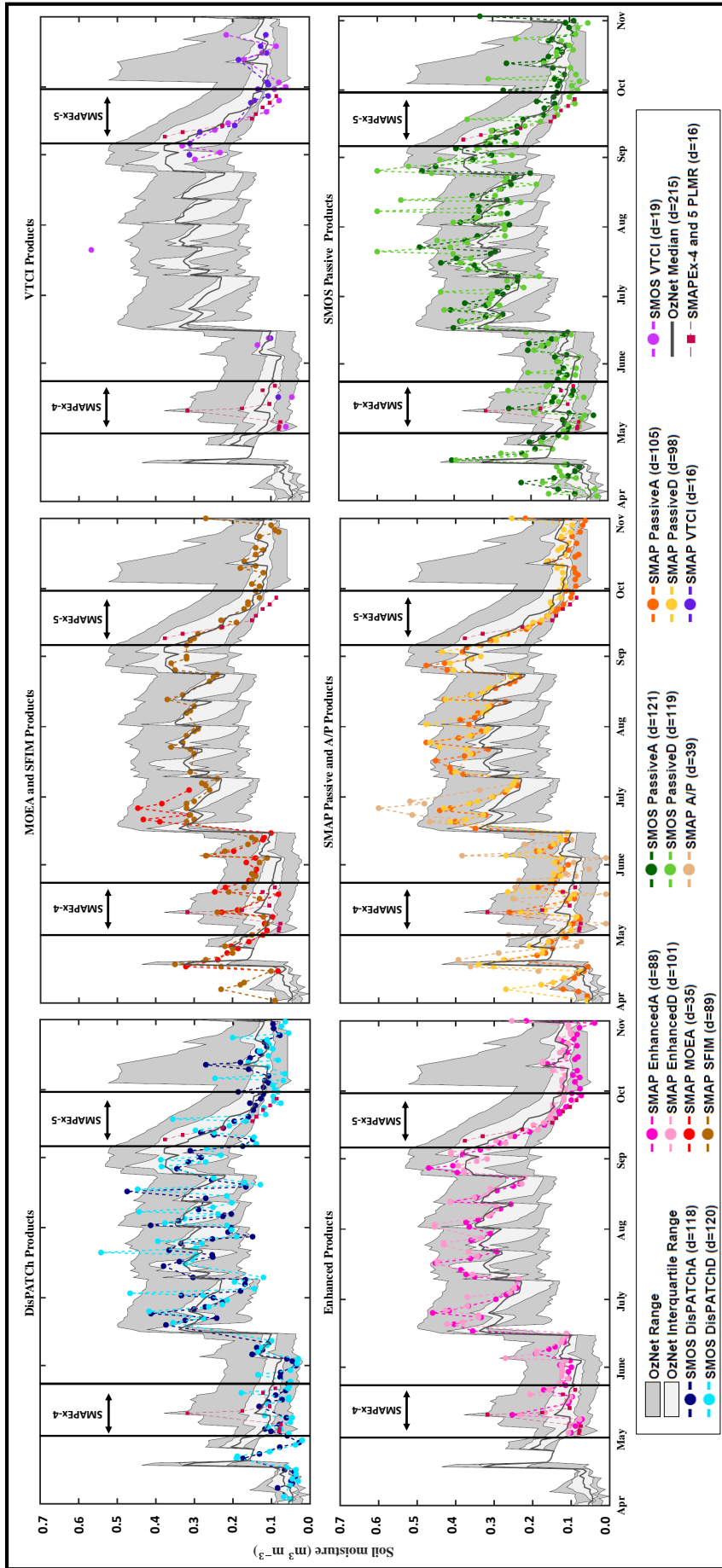


Figure 8: Sample of the temporal evolution of PLMR observed reference soil moisture estimates for 9 and 10 km pixels having the maximum *in situ* monitoring stations (shown in Figure 5). Shown here is the median of measurements from the OzNet stations, coarse SMAP and SMOS soil moisture retrievals posted to 9 km without any downscaling technique being applied, and the range of downscaled soil moisture estimates for the Yanco region during the period between 1 April and 1 November 2015; d indicates the number of days for which downscaled soil moisture products were available over the SMAPEX-4 and -5 flight area.

411 soil moisture estimates. While the SMAP Passive soil moisture estimates shown in Figure 8
412 were shown to be less than $0.47 \text{ m}^3 \text{ m}^{-3}$, the SMAP A/P soil moisture estimate on late June
413 2015 was shown to be more than $0.5 \text{ m}^3 \text{ m}^{-3}$. This is explained as follows: if the 36 km SMAP
414 Passive soil moisture is $0.47 \text{ m}^3 \text{ m}^{-3}$, as in this case, it is expected that some downscaled pixels
415 at higher spatial resolution will get wetter while some will get drier to compensate and maintain
416 the same average value as the coarser pixel.

417 This analysis assessed the accuracy of downscaled soil moisture products regardless of sub-
418 pixel surface heterogeneity and land cover types across the Yanco region, as downscaling tech-
419 niques should be applicable for a wide range of surface and vegetation cover conditions if they
420 are to be applied operationally. However, the dominant vegetation cover at 1 and 9 km spatial
421 resolution for the SMAPEX-4 and -5 airborne field campaigns are available in Figure A1 of the
422 Appendix to provide detailed information about vegetation cover over the study area.

423 **5.1 Temporal analysis against OzNet**

424 Temporal analysis of soil moisture products was carried out against pixels containing multiple
425 OzNet stations. In this analysis, time series of soil moisture values from the chosen pixels were
426 compared against corresponding values from aggregated OzNet soil moisture measurements. A
427 summary of accuracy statistics from different downscaled products is presented as a boxplot in
428 Figure 9, containing the minimum, maximum, median, and interquartile ranges together with
429 the mean.

430 **Evaluation of products at 1 km**

431 When compared against aggregated OzNet measurements at 1 km (Figure 9-a), the products
432 were shown to have a poorer performance than the products at 9 km. Such a decrease in the
433 performance of products at 1 km could be associated with the spatial-scale mismatch, which
434 is expected to be larger for higher resolution products (van der Velde et al., 2012). Moreover,

435 it has previously been noted by Yee et al. (2016) that the evaluation of soil moisture products
436 against OzNet stations in the Yanco region is indicated a better accuracy for coarser resolutions
437 whereby multi-stations are aggregated for each pixel footprint.

438 The SMAP VTCI with mean R^2 of 0.85 and mean RMSD of $0.07 \text{ m}^3 \text{ m}^{-3}$ was found to have
439 the best performance. The R^2 of DisPATCh products at 1 km were observed to be slightly
440 lower than that of DisPATCh products at 9 km. The same observation was made regarding the
441 R^2 of SMAP VTCI at 1 km, which did not change much in comparison with that of SMAP
442 VTCI at 9 km; the R^2 for 1 km scaled SMAP VTCI was on average 0.05 less than that of 9 km
443 SMAP VTCI. Conversely, the R^2 of SMOS VTCI at 1 km was observed to be roughly the same
444 as that of SMOS VTCI at 9 km; similar results were obtained for the SMOS PassiveD from
445 which SMOS VTCI originated. This similarity between the performance of SMOS PassiveD
446 and SMOS VTCI is consistent with previous results reported in Peng et al. (2015, 2016), which
447 showed that VTCI-based downscaled products maintained the accuracy of the original coarse
448 soil moisture products from which they were derived.

449 Except for SMOS VTCI at 1 km, which slightly underestimated OzNet soil moisture by
450 $-0.004 \text{ m}^3 \text{ m}^{-3}$ on average, the remaining products overestimated by between 0.012 and 0.046
451 $\text{m}^3 \text{ m}^{-3}$ on average. Underestimation of VTCI-based downscaled soil moisture products was also
452 reported by Peng et al. (2015, 2016). With the exception of SMAP VTCI, no improvement of
453 statistical parameters was observed for the 1 km downscaled products over the original coarse
454 passive SMAP and SMOS soil moisture measurements. However, the accuracy of DisPATChD
455 and SMOS VTCI were shown to be close to that of SMOS PassiveD.

456 Spatial resolution improvement of downscaled soil moisture products to even higher spatial
457 scale (such as field scale) is not expected to increase the accuracy. For example, Wu et al.
458 (2016) applied the active/passive optional (Das et al., 2011), baseline (Das et al., 2014) and
459 change detection (Piles et al., 2009) retrieval algorithms to the SMAPEX-3 airborne simulation
460 (Wu et al., 2015) of the SMAP data stream to test the robustness of alternate radar-radiometer

461 combination algorithms over a semi-arid region. From these alternate downscaling techniques,
462 downscaled soil moisture products were retrieved at three different spatial scales including 1,
463 3, and 9 km. Findings of this study revealed that all of the downscaled products at 9 km had
464 better performance than the products at 1 and 3 km spatial resolution in terms of RMSD and
465 spatial resolution improvement, with the downscaled products from 9 to 1 km deteriorating the
466 statistical metrics.

467 As suggested by Merlin et al. (2015), the slope of linear regression between downscaled
468 products and OzNet *in situ* measurements was also considered as an evaluation metric for
469 assessment of products at 1 and 9 km. However, the mean slope values of products at 1 km
470 varied between 1 and 1.3, showing little difference in the performance of products.

471 **Evaluation of products at 9 km**

472 Comparison of products at 9 km resolution (Figure 9-b) shows that the SMAP VTCI soil
473 moisture product had the best temporal agreement with OzNet measurements, followed by the
474 SMAP EnhancedD and EnhancedA products. The SMOS VTCI, SMOS PassiveD and Dis-
475 PATCHD had the lowest agreement with the temporal pattern of OzNet soil moisture compared
476 to other products at 9 km, having an average R^2 of ~ 0.6 . The difference between the perfor-
477 mance of the SMAP and SMOS VTCI is the result of the difference in the SMAP and SMOS
478 PassiveD from which the SMAP and SMOS VTCI products were derived. The SMAP VTCI
479 soil moisture had an overall bias of $-0.011 \text{ m}^3 \text{ m}^{-3}$, which explains the slight underestimation
480 relative to the ground OzNet measurements. While the SMOS VTCI, DisPATCHD and SMAP
481 VTCI underestimated relative to OzNet measurements, the other products overestimated. For
482 example, the SMAP MOEA with average bias of $0.057 \text{ m}^3 \text{ m}^{-3}$ had the most noticeable overes-
483 timation.

484 With the exception of SMAP VTCI and the Enhanced products, other downscaled products
485 at 9 km showed a deterioration in the R^2 when compared with the coarse original SMAP soil

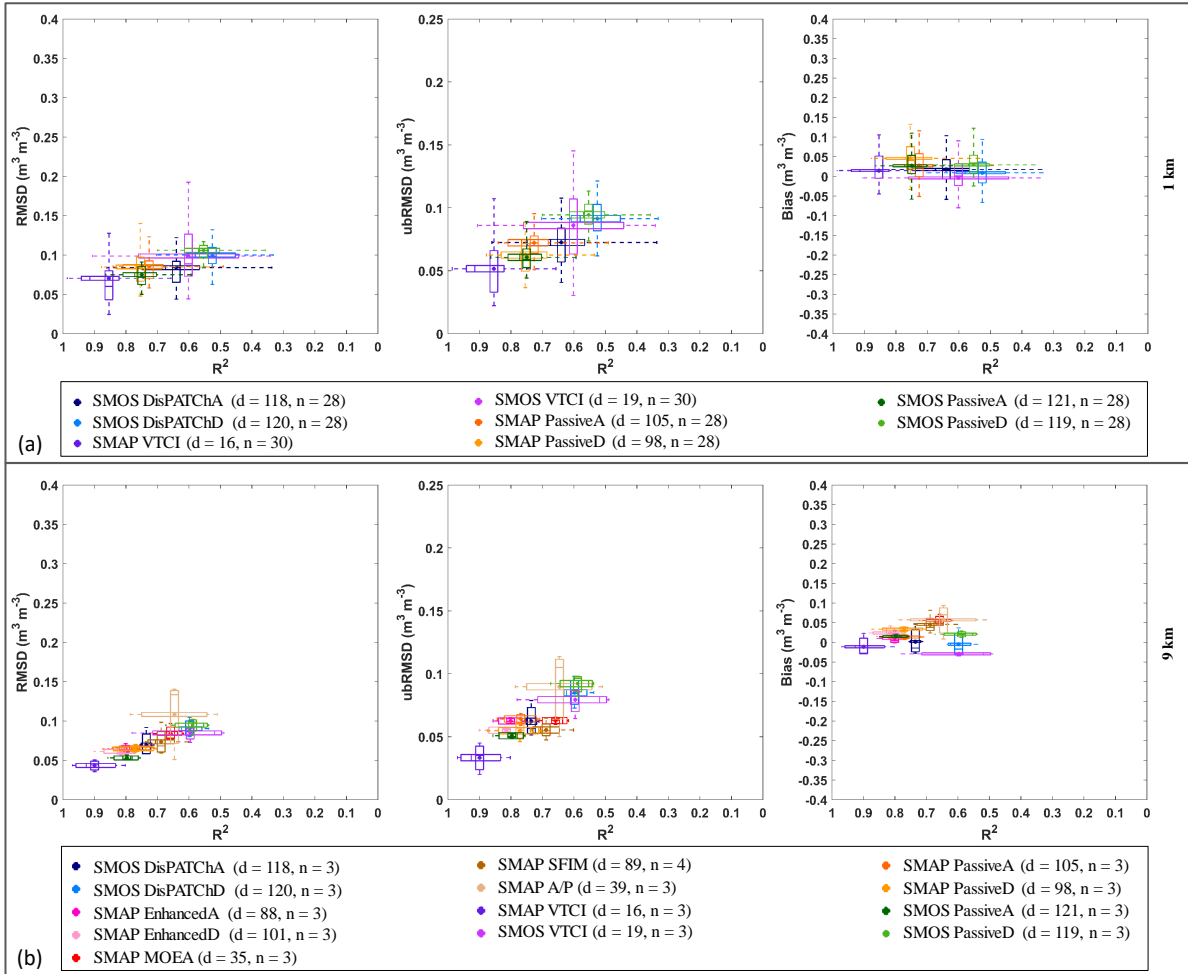


Figure 9: Summary of results obtained from temporal analysis of soil moisture products at (a) 1 km and (b) 9 km against OzNet. For 9 km products, only pixels with the largest number of stations were chosen. Each boxplot displays the distribution of the accuracy statistics of different downscaled products based on the interquartile range, the maximum and minimum range, and the statistics median (bar) associated with the mean (dot). d indicates the number of downscaled products that were used in this analysis and n indicates the number of statistical parameters that are summarized in this figure.

486 moisture products. For instance, the R^2 of SMAP A/P was on average 0.12 less than that of
 487 SMAP PassiveA and PassiveD. Inferiority of SMAP A/P to SMAP Passive products in terms
 488 of temporal correlation with *in situ* measurements has also been reported by Mishra et al.
 489 (2018), who evaluated SMAP A/P Level 3 soil moisture products using *in situ* soil moisture
 490 measurements from the Soil Climate Analysis Network (SCAN) stations across the Continental
 491 United States. The temporal correlation between the SMAP SFIM and *in situ* OzNet soil
 492 moisture measurements also tended to be lower than that of the SMAP Passive soil moisture
 493 products, similar to results reported by Gevaert et al. (2015).

494 Among the downscaled products, the SMAP EnhancedA and EnhancedD downscaled prod-
495 ucts maintained a similar RMSD to the coarse SMAP passive soil moisture products. It is to
496 be noted that SMAP VTCI was the only downscaled product which outperformed the original
497 coarse passive SMAP in terms of RMSD, hitting the lowest values of RMSD and ubRMSD.
498 The DisPATChD could not improve the accuracy of non-downscaled SMOS PassiveD from
499 which DisPATChD originated. However, the DisPATChD showed a close performance to that
500 of SMOS PassiveD.

501 The SMAP EnhancedD with mean R^2 of 0.81, mean RMSD of $0.061 \text{ m}^3 \text{ m}^{-3}$ and mean bias
502 of $0.024 \text{ m}^3 \text{ m}^{-3}$ was found to have a slightly better performance than the SMAP EnhancedA.
503 The performance of the Enhanced product was generally consistent with that of the evaluation
504 by Chan et al. (2018) who assessed the performance of the Enhanced products for the period
505 April 1, 2015 to October 30, 2016 using *in situ* data from the SMAP mission core validation
506 sites including Yanco. Chan et al. (2018) reported on the similarity between the performance of
507 Enhanced products and that of SMAP passive soil moisture products. Based on their analysis,
508 the SMAP EnhancedD data attained a mean R^2 of 0.92 (correlation coefficient/ $R = 0.96$), mean
509 RMSD of $0.048 \text{ m}^3 \text{ m}^{-3}$ and mean bias of $0.02 \text{ m}^3 \text{ m}^{-3}$ with *in situ* stations over the Yanco re-
510 gion. Li et al. (2018) evaluated the accuracy of the SMAP EnhancedD against two ground-based
511 soil moisture and temperature monitoring networks located in the Tibetan Plateau, likewise re-
512 ported on the reliability of the SMAP EnhancedD products in capturing the temporal variations
513 of soil moisture. Li et al. (2018) reported small values of ubRMSE ($0.055\text{--}0.059 \text{ m}^3 \text{ m}^{-3}$) and
514 high temporal correlation coefficients ($0.64\text{--}0.88$) for Enhanced Products.

515 Similar to slope analysis for products at 1 km, there was no substantial statistical difference
516 between the mean slope values for products at 9 km; with the range of mean slope being between
517 0.9 and 1.4. A slope larger than 1 could be attributed to the difference between the sensing
518 depth of downscaled products (varying between 0 and 5 cm) and that of *in situ* measurements
519 being 0-5 cm.

520 An unequal number of soil moisture values were analysed for the different products included
521 in the temporal analysis against the OzNet stations, due to the availability of product retrievals.
522 This may raise a concern about the impact of the unequal number of data used in the estimation
523 of statistical metrics, and thus the findings from the analysis. Consequently, the temporal
524 analysis was also conducted for a consistent number of data by using only observations on
525 the same dates (eight days only). This included comparison of SMAP EnhancedD, SMAP
526 SFIM, SMAP PassiveD, SMOS PassiveD, SMAP VTCI and SMOS VTCI against the OzNet
527 measurements. Findings from this analysis were consistent with the earlier results. However,
528 the statistical metrics of the eight days only scenario were deteriorated compared to those
529 summarized in Figure 9. Still, the SMAP VTCI at both 1 and 9 km were found to have
530 the best performance. For the comparisons conducted at 1 km, the SMAP PassiveD followed
531 closely the SMAP VTCI. Results obtained from the analysis of products at 9 km revealed that
532 the performance of SMAP VTCI was followed by that of the SMAP EnhancedD and SMAP
533 PassiveD.

534 **General results**

535 In the case of temporal analysis of downscaled products at 9 km against OzNet (Figure 13),
536 SMAP EnhancedA and EnhancedD products were generally superior to other downscaled prod-
537 ucts. Both reached the highest temporal correlation with OzNet and had the lowest bias. SMAP
538 VTCI at 1 km resolution also showed superiority to the remaining downscaled products at 1
539 km.

540 **5.2 Temporal analysis against airborne PLMR soil moisture**

541 **Evaluation of products at 1 km**

542 The temporal analysis of products was also carried out against the entire airborne PLMR soil
543 moisture maps captured over the SMAPEX-4 and -5 airborne field campaigns. A summary of

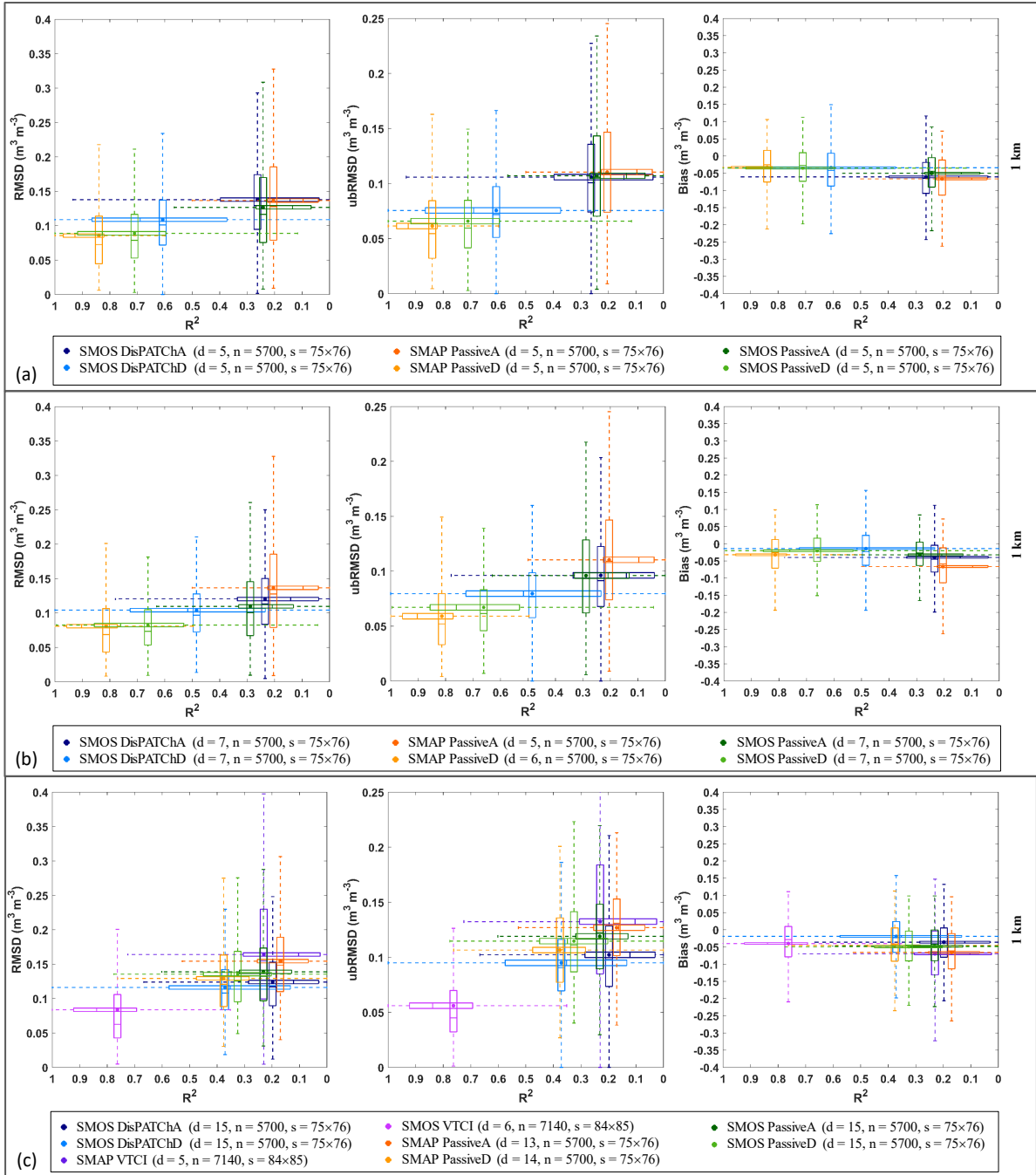


Figure 10: As for Figure 9 but for the comparison against airborne PLMR soil moisture at 1 km in which analysis was carried out for all the pixels covering the study area. These results are from different scenarios including: a) the equal number of downscaled products captured during SMAPEX-4, b) all available products during the SMAPEX-4, and c) products captured over the entire SMAPEX-4 and -5 airborne field campaigns' period. Here s stands for the dimension of analysis area arranged in $row \times column$. Note: the performance analysis of the VTCI-based products was not possible for the SMAPEX-4 period as only one SMOS VTCI and two SMAP VTCI soil moisture maps were available.

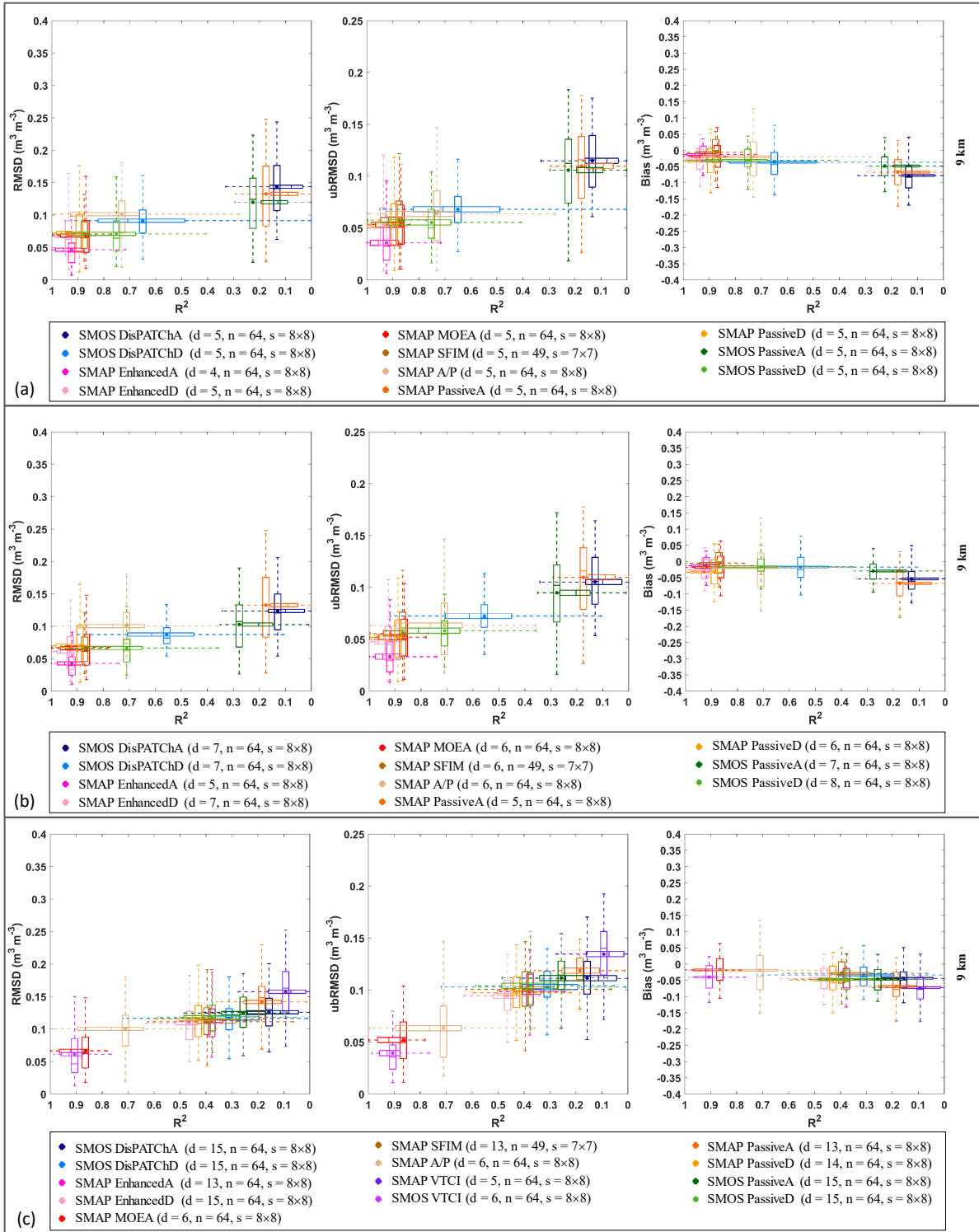


Figure 11: As for Figure 10 but for the comparison against airborne PLMR soil moisture at 9 km.

544 product accuracy statistics at 1 and 9 km resolution are presented as boxplots in Figures 10 and

545 11, respectively. When the same number of downscaled and non-downscaled soil moisture maps

546 at 1 km (Figure 10-a) were evaluated, descending SMAP and SMOS coarse passive products
547 showed superiority in terms of accuracy when contrasted with the downscaled products, having
548 a mean $R^2 \geq 0.6$ and mean RMSD of $\sim 0.09 \text{ m}^3 \text{ m}^{-3}$. The SMOS DisPATChD maintained
549 a similar accuracy to that of SMOS PassiveD, and performed the best among the downscaled
550 products. Generally, all products underestimated the airborne PLMR soil moisture; with the
551 underestimation being greater in the SMAP PassiveA and SMOS DisPATChA.

552 For the comparison against SMAPEX-4 and -5 airborne field campaigns (Figure 10-c), SMOS
553 VTCI at 1 km performed the best with R^2 of 0.76, RMSD of $0.084 \text{ m}^3 \text{ m}^{-3}$ and ubRMSD of
554 $0.056 \text{ m}^3 \text{ m}^{-3}$, which were better statistical metrics than for the other products. This was
555 followed by the SMOS DisPATChD and SMAP PassiveD products which performed similarly;
556 with a mean R^2 close to 0.4, mean RMSD of about $0.12 \text{ m}^3 \text{ m}^{-3}$ and mean bias between
557 0 and $-0.05 \text{ m}^3 \text{ m}^{-3}$. It is to be noted that the maximum R^2 for both SMOS VTCI and
558 DisPATChD was equal to 1, while other products could not reach this high level of temporal
559 agreement with airborne PLMR soil moisture. The slope of the linear regression defined between
560 downscaled products and PLMR soil moisture maps showed dependency to R^2 . As anticipated,
561 the slope values were small (close to zero) for products that had low R^2 . The slope was mainly
562 explained by the correlation, knowing that slope equals to $(\text{correlation}) \times (\text{standard deviation of}$
563 $\text{downscaled products} / \text{standard deviation of reference data})$. Therefore, the standard deviation
564 of downscaled products was rather similar across all products. Comparison of SMOS VTCI
565 and SMOS DisPATCh as optical-based products has also been conducted for the SMAPEX-4
566 and -5 airborne field campaigns, by choosing the same dates. Based on this comparison, the
567 performance of DisPATCh and VTCI was quite comparable.

568 **Evaluation of products at 9 km**

569 At 9 km resolution for the scenario in which the same number of soil moisture maps were eval-
570 uated (Figure 11-a), the SMAP EnhancedA and EnhancedD products with average R^2 of 0.92

571 and 0.94, respectively, surpassed the other downscaled soil moisture products in capturing the
572 temporal evolution of airborne soil moisture estimates, followed by SMAP PassiveD, SFIM and
573 MOEA. The SMOS PassiveD and SMAP A/P products also showed a good performance with
574 R^2 of 0.75 for the first and 0.73 for the later. The SMAP PassiveD without being downscaled
575 was amongst the best results and yielded an R^2 of 0.89 and ubRMSD of $0.054 \text{ m}^3 \text{ m}^{-3}$. Nev-
576 ertheless, the SMAP EnhancedA was found to have the best agreement with airborne PLMR
577 soil moisture. The SMAP EnhancedA not only had a high coefficient of determination but
578 also low RMSD and/or ubRMSD. The DisPATChA at 9 km - retrieved from an optical-based
579 downscaling technique - had the lowest agreement with airborne PLMR soil moisture. This is
580 unlike the DisPATChD which was shown to have a moderate performance with R^2 of 0.75. The
581 DisPATChD yielded on average similar performance to the SMOS PassiveD. While it did not
582 improve nor maintain the accuracy of SMOS PassiveD in terms of RMSD and ubRMSD, it de-
583 teriorated the R^2 and bias relative to SMOS PassiveD. Nevertheless, the R^2 of SMOS PassiveD
584 was not significantly above that of DisPATChD. These findings are in agreement with those
585 obtained from evaluation of all available soil moisture products during the SMAPEX-4 (Figure
586 11-b).

587 For the comparison against SMAPEX-4 and -5 airborne field campaigns (Figure 11-c), SMOS
588 VTCI at 9 km performed the best with a mean R^2 of 0.91, mean bias of $-0.04 \text{ m}^3 \text{ m}^{-3}$, mean
589 RMSD of $0.061 \text{ m}^3 \text{ m}^{-3}$, and mean ubRMSD of $0.039 \text{ m}^3 \text{ m}^{-3}$ followed by SMAP MOEA and
590 A/P, which were only available for the SMAPEX-4 period. The remaining products, with the ex-
591 ception of the SMAP VTCI, SMOS DisPATChA and SMAP PassiveA, had similar performance
592 with mean R^2 between 0.2 and 0.5 and varying RMSD between 0.1 and $0.13 \text{ m}^3 \text{ m}^{-3}$.

593 **Seasonal performance of products at 1 km**

594 In order to assess the seasonal impact on the performance of products at 1 km, the temporal
595 analysis of products was also carried out for the SMAPEX-5 airborne field campaign conducted

596 in the austral spring. During the SMAPEX-5 with wet soils, the products again underesti-
597 mated the airborne PLMR soil moisture, being even more severe than for SMAPEX-4. This
598 underestimation could be the result of standing water in some fields and the denser vegetation
599 cover in cropping areas during SMAPEX-5. The performance of SMOS DisPATChD, SMAP En-
600 hancedD, SMAP EnhancedA and SMAP PassiveD during SMAPEX-5 showed a minor difference
601 over their performance during SMAPEX-4 in terms of R^2 and ubRMSD. With the exception of
602 SMOS PassiveD, whereby R^2 decreased marginally from 0.66 (SMAPEX-4) to 0.57 (SMAPEX-
603 5), the R^2 of remaining products during SMAPEX-5 increased by more than 0.5 compared to
604 that of SMAPEX-4. The SMAP PassiveA products experienced the largest increase (0.68) in
605 terms of R^2 and had the lowest agreement with SMAPEX-4 PLMR soil moisture. More ex-
606 plicit spatial and temporal patterns of soil moisture were observed in the PLMR derived maps
607 during the SMAPEX-5 than the SMAPEX-4 airborne field campaign, as shown in Figure 6 and
608 7. Therefore, it was expected that the downscaled products would best capture the explicit
609 spatial and temporal variability of soil moisture during the SMAPEX-5 airborne field campaign.
610 Results from the comparison of SMOS VTCI and SMOS DisPATCh on the same dates during
611 the SMAPEX-5 airborne field campaign revealed a similarity of DisPATCh and VTCI in terms
612 of performance.

613 For the comparison against SMAPEX-5 airborne field campaign data, with the exception of
614 SMOS PassiveD and DisPATChD with R^2 less than 0.6, the remaining products were found
615 to have an R^2 greater than 0.75. The SMOS DisPATChA had a reasonable performance with
616 an R^2 of 0.77, a lower bias ($-0.033 \text{ m}^3 \text{ m}^{-3}$) and a lower ubRMSD ($0.044 \text{ m}^3 \text{ m}^{-3}$) than other
617 products. This is unlike the SMOS VTCI, SMAP VTCI, SMAP PassiveA, SMAP PassiveD,
618 and SMOS PassiveA, which with $R^2 \geq 0.85$ could not meet the accuracy requirements in terms
619 of bias and RMSD. For instance, the SMOS VTCI had the largest bias equal to $-0.115 \text{ m}^3 \text{ m}^{-3}$
620 on average and the largest RMSD equal to $0.143 \text{ m}^3 \text{ m}^{-3}$ on average.

621 **Seasonal performance of products at 9 km**

622 The seasonal performance assessment was also carried out for the products at 9 km. Based on
623 this comparison, with the exception of SMOS PassiveD, SMOS DisPATChA and DisPATChD,
624 the remaining products were superior with an $R^2 \geq 0.9$. This is not in line with the findings from
625 the SMAPEX-4 in which SMOS PassiveA, SMOS DisPATChA and SMAP PassiveA had an R^2
626 less than 0.3. Generally, the variation of RMSD, ubRMSD, and bias obtained from evaluation
627 of 9 km products during the SMAPEX-5 was found to be smaller than that of products at 1 km.
628 Still, the average of obtained statistical metrics for 9 km products was quite similar to that of
629 products at 1 km.

630 Generally, a comparison of the temporal performance of DisPATCh products against air-
631 borne PLMR soil moisture showed that the accuracy of DisPATCh products was noticeably
632 affected by that of the SMOS Passive products. While DisPATCh products were not superior
633 to SMOS Passive products in terms of R^2 , the DisPATCh products were shown to mimic the
634 SMOS Passive R^2 . For example, the SMOS PassiveA and SMOS PassiveD at 9 km had an
635 average R^2 of 0.9 and 0.63, respectively, during the SMAPEX-5, with DisPATChA and Dis-
636 PATChD showing an average R^2 of 0.8 and 0.5 for the former and latter. Results herein have
637 also shown that DisPATCh products had a higher RMSD/ubRMSD than SMOS Passive prod-
638 ucts during SMAPEX-4, which is opposite to the results obtained for the SMAPEX-5 period.
639 During SMAPEX-5 the RMSD of DisPATCh products were slightly lower than those of the
640 SMOS Passive products.

641 **General results**

642 Analysis of downscaled products against airborne PLMR soil moisture maps revealed the supe-
643 riority of the oversampling-based technique in terms of delivering more frequent and accurate
644 downscaled products than the radar-, optical- and radiometer-based techniques. The SMAP
645 Enhanced products not only had better performance and availability, but also showed improve-

646 ment over coarse SMAP radiometer only soil moisture products in terms of accuracy and spatial
647 scale.

648 **Spatial analysis against airborne PLMR soil moisture**

649 Spatial analysis of soil moisture products was carried out against airborne PLMR soil moisture
650 maps covering the entire study area during the SMAPEX-4 and -5 airborne field campaigns.
651 This spatial analysis involved evaluation of the daily maps of soil moisture estimates against
652 the corresponding airborne PLMR maps in the same scenarios as in the temporal analysis. A
653 summary of the spatial accuracy statistics of products at 1 and 9 km are presented as boxplots
654 in Figures 12 and 13, respectively.

655 **Evaluation of products at 1 km**

656 When downscaled soil moisture maps at 1 km were evaluated (Figure 12), they showed low
657 spatial correlation, denoted by R^2 , with airborne PLMR maps. Such a low spatial correlation
658 was followed by low linear regression slope. In the spatial analysis, the spatial correlation
659 was very low for all products, with the slope mainly determined by the standard deviation of
660 downscaled products in space. Furthermore, they underestimated the variability of the PLMR
661 soil moisture with the range of average bias between -0.016 and $-0.075 \text{ m}^3 \text{ m}^{-3}$. For the scenarios
662 including: i) evaluation of the same number of products (Figure 12-a) and ii) evaluation of
663 products during the SMAPEX-4 (Figure 12-b), the products had a mean R^2 of less than 0.2 and
664 the range of mean RMSD between 0.083 and $0.146 \text{ m}^3 \text{ m}^{-3}$. These results in general are not
665 much different from those of comparisons against SMAPEX-4 and -5 airborne field campaigns
666 (Figure 12-c). However, results in Figure 12-c showed closer resemblance in the performance of
667 products compared to Figure 12-a and b.

668 **Evaluation of products at 9 km**

669 In the case of spatial pattern analysis of products at 9 km (Figure 13), generally, SMAP En-
670 hancedA and EnhancedD products were superior to other products. Both reached the highest
671 spatial correlation with airborne PLMR soil moisture and had the lowest bias. Nevertheless,
672 the SMAP Enhanced products had mean R^2 less than 0.5 and mean bias larger than 0.04 m^3
673 m^{-3} . In addition, the slope of linear regression between SMAP Enhanced products and PLMR
674 soil moisture was close to 0.1. The slope was mainly determined by the standard deviation of
675 downscaled products in space, which is expected to be lower for coarser/lower resolutions. The
676 SMAP A/P showed the highest variability in terms of slope range, and SMAP EnhancedA was
677 one of the products with the lowest variability. Apart from the Enhanced products, the SFIM
678 performance was shown to be one of the best during the short SMAPEX-4 period.

679 **Seasonal performance of products at 1 km**

680 Comparison of the performance of products at 1 km during the SMAPEX-5 (austral spring)
681 against that of products during the SMAPEX-4 (austral autumn) showed that there was no
682 noticeable seasonal impact on the spatial performance of products. None of the products at
683 1 km could capture the spatial pattern of PLMR soil moisture with high correlation and low
684 RMSD. Agreeing with findings from the evaluation of products during the SMAPEX-4 period,
685 the mean R^2 of products was generally less than 0.1 and mean RMSD was higher than 0.09 m^3
686 m^{-3} for SMAPEX-5. Regardless of season, there was an underestimation of PLMR soil moisture
687 by products with a more noticeable error in the SMAPEX-5 period.

688 **Seasonal performance of products at 9 km**

689 In contrast to the seasonal performance of products at 1 km, the seasonal impact on the spatial
690 performance of products at 9 km was noticeable. Products at 9 km showed slightly better
691 performance during SMAPEX-4 than during SMAPEX-5 when soils were wet. Comparison of

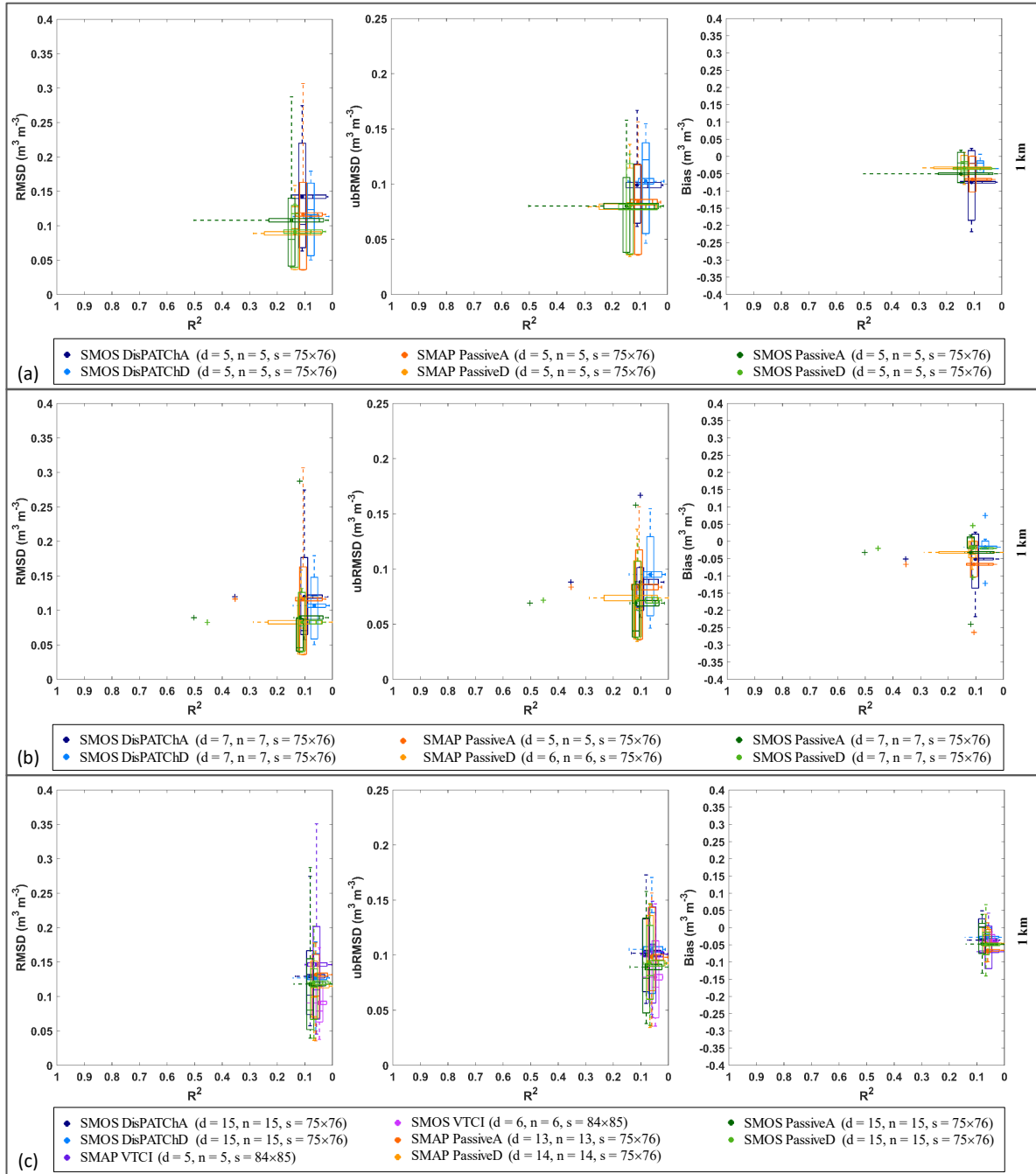


Figure 12: Summary of results obtained from spatial analysis of soil moisture products at 1 km against airborne PLMR soil moisture in which analysis was carried out for all the pixels covering the study area. These results are from different scenarios including: a) the equal number of downscaled products captured during SMAPEX-4, b) all available products during the SMAPEX-4, and c) products captured over the entire SMAPEX-4 and -5 airborne field campaigns' period.

692 the correlation of products with PLMR soil moisture during SMAPEX-5 with that of products
 693 during SMAPEX-4 showed a reduction of R^2 for SMAPEX-5, which was more pronounced for
 694 the SMAP SFIM. The SMAP SFIM was among products with the best performance during

695 SMAPE_x-4, but among those with the poorest performance during SMAPE_x-5. The SMAP
696 SFIM experienced a decrease in R^2 from 0.33 in SMAPE_x-4 to 0.14 in SMAPE_x-5 and increase
697 of RMSD from 0.062 to 0.093 $\text{m}^3 \text{m}^{-3}$. Although the performance of SMAP EnhancedA was
698 slightly poorer during SMAPE_x-5 than SMAPE_x-4, it still ranked the best with R^2 of 0.18,
699 RMSD of 0.089 $\text{m}^3 \text{m}^{-3}$ and ubRMSD of 0.055 $\text{m}^3 \text{m}^{-3}$.

700 General results

701 Based on the results, none of the downscaled products could capture the spatial variability of
702 the PLMR soil moisture maps. Products at both 1 and 9 km showed low spatial correlation
703 with airborne PLMR maps, denoted by R^2 values less than 0.5. However, products at 1 km had
704 a lower spatial correlation than the products at 9 km, with R^2 values of ~ 0.1 . While none of
705 these methods met the accuracy expectations, the slightly better results at 9 km were expected,
706 being an artefact of undertaking the evaluation at larger spatial scales where the high spatial
707 variability is smoothed by the averaging processes.

708 Superiority of the oversampling-based technique to the radar-, optical- and radiometer-
709 based techniques, in capturing spatial variability of airborne PLMR soil moisture, was revealed
710 based on findings from spatial analysis. Nevertheless, the oversampling-based products did
711 not indicate a strong correlation with the airborne PLMR spatial pattern. The superiority of
712 the oversampling-based product relative to others was not limited to just the spatial patterns
713 provided by airborne PLMR soil moisture maps; temporal evaluation against the *in situ* soil
714 moisture measurements and airborne PLMR soil moisture estimates also revealed superiority
715 of the oversampling-based products. For both of the temporal analyses, oversampling-based
716 products had a low RMSD/ubRMSD and high R^2 values. Availability of the oversampling-
717 based products under all-weather conditions is another factor supporting their adoption for
718 applications.

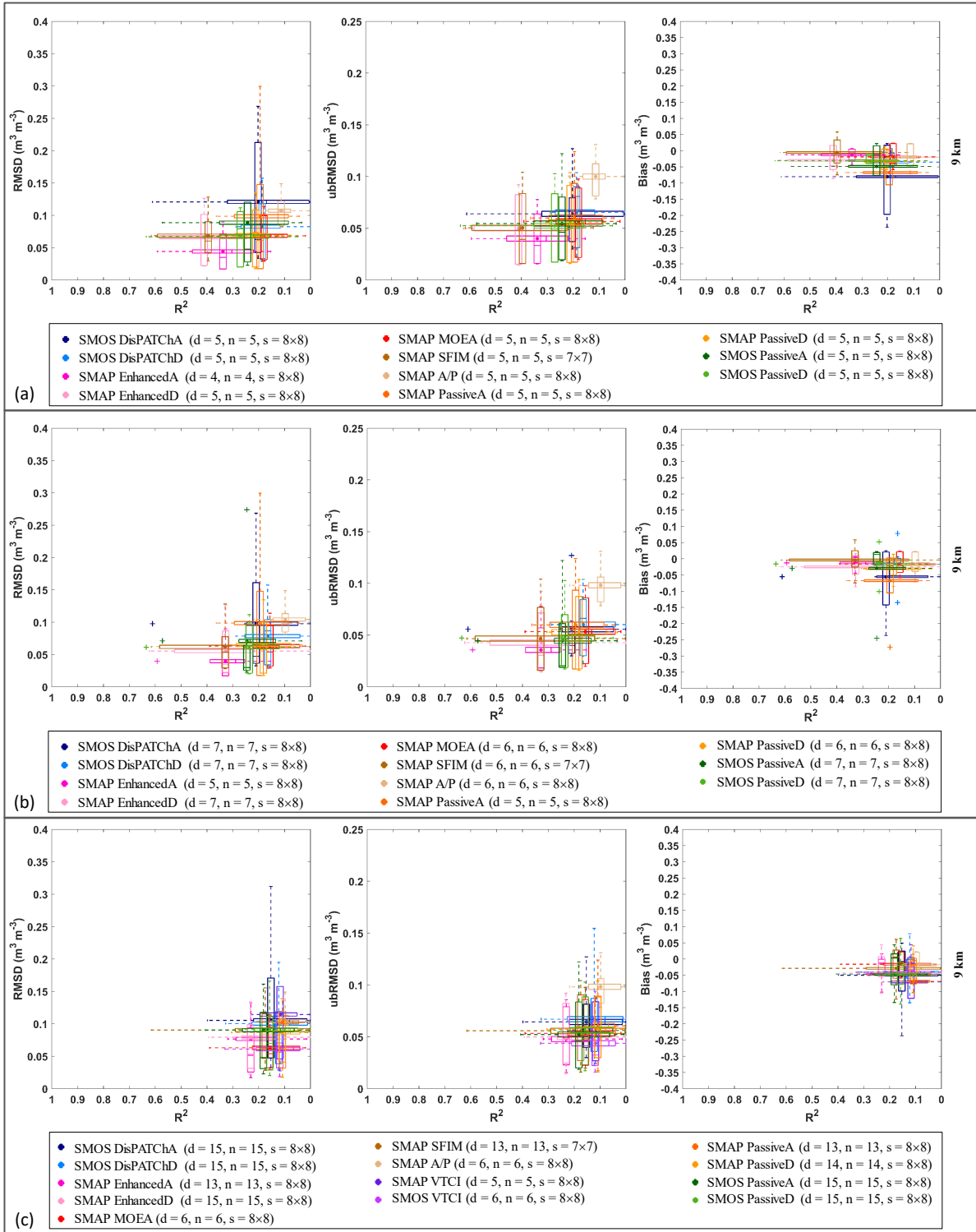


Figure 13: As for Figure 12 but for the spatial analysis at 9 km.

719 **6 Discussion**

720 This paper has rigorously assessed the performance of a variety of available downscaled soil
721 moisture products at resolutions between 1 and 10 km, to find approach(es) that is(are) ap-
722 plicable for multi-sensor soil moisture retrieval from the SMAP and SMOS. This assessment
723 involved comprehensive inter-comparison of downscaled products, including radar-, optical-,
724 radiometer- and oversampling-based retrievals against *in situ* and airborne reference data for a
725 typical Australian landscape and climate. The performance of the original coarse radiometer
726 only products including SMAP and SMOS was analyzed to understand the extent of improve-
727 ment of their respective downscaled products in terms of accuracy and capability of capturing
728 the spatio-temporal variability of soil moisture relative to assuming a uniform spatial field. A
729 summary of accuracy statistics of the downscaled and non-downscaled products at 9 km, eval-
730 uated against the airborne PLMR soil moisture during SMAPEX-4 and -5, and OzNet *in situ*
731 soil moisture measurements is provided in Table 2. Based on Table 2, none of the products at
732 9 km could deliver soil moisture estimates at an accuracy of $0.04 \text{ m}^3 \text{ m}^{-3}$, being the accuracy
733 requirement suggested for a wide range of soil moisture applications over areas with vegetation
734 water content of less than 5 kg.m^{-2} (Entekhabi et al., 2008).

735 Based on the results, downscaled products showed a range of performance against differ-
736 ent reference data sets and under differing spatial scale, weather and climate condition. This
737 variation of performance between downscaled products could be influenced by the nature of uti-
738 lized ancillary data for downscaling purpose. For example, in Figure 6 and 7 the optical-based
739 products could not retrieve consistent time series of soil moisture maps under cloudy skies as
740 optical observations are not captured under cloud coverage. This shortcoming reduces the func-
741 tionality of optical-based techniques while the high temporal and spatial resolution of optical
742 observations make them a promising ancillary data for soil moisture downscaling. Studies such
743 as Zhao and Li (2013), Peng et al. (2015), Piles et al. (2016), and Sabaghy et al. (2018) have

Table 2: Averaged accuracy of the downscaled and non-downscaled products at 9 km, evaluated against the airborne PLMR soil moisture and OzNet *in situ* soil moisture measurements. Notes: i) the evaluation of SMAP MOEA and A/P was only carried out during the short SMAPEX-4 period due to radar availability, and ii) gray cells indicate the accuracy of products with superior performance to the other downscaled products.

Downscaling Technique	Downscaled Product	Temporal analysis against airborne				Spatial analysis against airborne				Temporal analysis against OzNet			
		PLMR during SMAPEX-4 and -5		PLMR during SMAPEX-4 and -5		PLMR during SMAPEX-4 and -5		PLMR during SMAPEX-4 and -5		PLMR during SMAPEX-4 and -5		PLMR during SMAPEX-4 and -5	
		Bias ($\text{m}^3 \text{m}^{-3}$)	R ²	RMSD ($\text{m}^3 \text{m}^{-3}$)	ubRMSD ($\text{m}^3 \text{m}^{-3}$)	Bias ($\text{m}^3 \text{m}^{-3}$)	R ²	RMSD ($\text{m}^3 \text{m}^{-3}$)	ubRMSD ($\text{m}^3 \text{m}^{-3}$)	Bias ($\text{m}^3 \text{m}^{-3}$)	R ²	RMSD ($\text{m}^3 \text{m}^{-3}$)	ubRMSD ($\text{m}^3 \text{m}^{-3}$)
Radar-based	SMAP MOEA	-0.018	0.86	0.066	0.052	-0.016	0.16	0.063	0.053	0.66	0.084	0.063	
	SMAP A/P	-0.019	0.71	0.100	0.063	-0.018	0.10	0.104	0.098	0.65	0.108	0.090	
Optical-based	SMOS DisPATCHA	-0.044	0.16	0.126	0.111	-0.050	0.15	0.105	0.064	0.002	0.71	0.072	
	SMOS DisPATCHD	-0.034	0.31	0.116	0.103	-0.040	0.12	0.100	0.067	-0.005	0.60	0.085	
	SMAP VTCI	-0.073	0.09	0.157	0.135	-0.071	0.12	0.114	0.056	-0.011	0.90	0.044	
	SMOS VTCI	-0.040	0.91	0.061	0.039	-0.040	0.12	0.061	0.044	-0.029	0.60	0.079	
Radiometer-based	SMAP SFIM	-0.028	0.40	0.111	0.101	-0.029	0.17	0.090	0.056	0.69	0.074	0.055	
Oversampling-based	SMAP EnhancedA	-0.047	0.38	0.113	0.098	-0.047	0.23	0.077	0.048	0.012	0.85	0.060	
	SMAP EnhancedD	-0.044	0.46	0.109	0.094	-0.043	0.23	0.079	0.050	0.024	0.81	0.061	
Uniform field	SMAP PassiveA	-0.069	0.19	0.142	0.119	-0.069	0.11	0.102	0.061	0.018	0.84	0.059	
	SMAP PassiveD	-0.049	0.43	0.116	0.097	-0.048	0.11	0.087	0.057	0.034	0.77	0.065	
	SMOS PassiveA	-0.046	0.26	0.125	0.112	-0.046	0.18	0.090	0.052	0.017	0.79	0.054	
	SMOS PassiveD	-0.047	0.38	0.118	0.104	-0.047	0.16	0.091	0.056	0.020	0.63	0.090	

744 suggested the use of geostationary based optical observations, instead of the optical imagery
745 captured by polar orbiting counterparts, to overcome this issue. The geostationary sensors
746 provide more frequent acquisitions and thus an opportunity for more cloud-free observations.
747 Furthermore, multi-sensor data fusion techniques could be employed as an alternative to the
748 use of geostationary based optical observations, in order to generate continuous time series of
749 cloud-free optical imageries (e.g. Long et al., 2019).

750 Unlike optical-based products, radar-, radiometer-, and oversampling-based downscaled soil
751 moisture maps were available regardless of meteorological conditions. Oversampling-based prod-
752 ucts retrieved from optimal interpolation theory, which provides the closest observation to what
753 could be measured by the radiometric instrument at the interpolation point, has the added ad-
754 vantage of not needing concurrent data from other sensors. This factor prevents data loss due
755 to unavailability of required ancillary data for disaggregation. The lack of access to concurrent
756 radar and radiometer observations that have the same temporal repeat is the main factor that
757 limits the application of the radar-based downscaling techniques.

758 The oversampling-based soil moisture products (SMAP EnhancedA and SMAP EnhancedD)
759 best captured the temporal and spatial variability of soil moisture overall, though the SMAP
760 MOEA and A/P had the better temporal agreement with PLMR during the short SMAPEX-4
761 period. This superiority may lie in the characteristic of the L-band radiometer and radar data
762 used for their soil moisture disaggregation. Especially, the oversampling-based soil moisture
763 products with their disaggregation procedure based on the use of SMAP L-band radiometer im-
764 ageries that are less affected by vegetation cover, surface roughness and meteorology condition.

765 The summary of accuracy statistics, in the review of temporal analysis of different down-
766 scaling techniques displayed in Figure 8 of Sabaghy et al. (2018), indicated that the radar-
767 based technique was expected to deliver more accurate downscaled soil moisture products than
768 optical-based techniques, with radar having been previously shown to have a greater sensitivity
769 to soil moisture dynamics than optical observation and with a direct relation to soil moisture

770 dynamics. Nevertheless, in this study the temporal analysis of products against the OzNet
771 ground-based soil moisture measurements revealed that optical-based products (SMAP VTCI
772 at 9 km) performed the best, followed by the oversampling-based product (SMAP EnhancedD).
773 The radiometer-based products which had the poorest performance in the review by Sabaghy
774 et al. (2018), herein showed reasonable performance, being slightly higher than that of radar-
775 based products (SMAP A/P and MOEA). Moreover, the temporal analysis of products against
776 the airborne PLMR soil moisture during SMAPEX-4 and -5 revealed that SMOS VTCI at 9 km
777 performed the best, followed by the radar-based products (SMAP A/P and MOEA).

778 Differences observed between the temporal analysis of products against *in situ* and airborne
779 soil moisture references suggest that relying only on *in situ* measurement is not appropriate
780 for validation of soil moisture maps; basically *in situ* measurements are not necessarily a great
781 indicator of soil moisture variation in space. Furthermore, *in situ* measurements are not consis-
782 tent and have station-to-station bias variations (Colliander et al., 2017). In addition, Yee et al.
783 (2016) recommended a need to identify the most representative station(s) based on evaluation
784 against intensive soil moisture measurements to avoid biases in the *in situ* measurements due
785 to station placement. While there are a few isolated locations where temporal evaluation was
786 possible using stations, the aircraft with its full spatial coverage created the opportunity to look
787 in detail at the spatial patterns.

788 Based on the temporal analysis of seasonal performance, the performance of SMOS PassiveA
789 and DisPATChA products were noticeably affected by the season. The 9 km SMOS PassiveA
790 and DisPATChA had mean $R^2 < 0.3$ during SMAPEX-4 and mean $R^2 \geq 0.8$ during SMAPEX-
791 5, while the average RMSD/ubRMSD and bias of these products was approximately the same
792 for both campaigns. Merlin et al. (2012) previously reported a similar impact of seasonal
793 variations on the accuracy of DisPATCh products in capturing the spatial dynamic of soil
794 moisture but with better temporal correlation of DisPATCh products against reference soil
795 moisture for summer (semi-arid climate) than winter (temperate climate). The downscaled

796 DisPATCh products were derived using the evaporative efficiency as the main downscaling
797 factor, which has a higher level of coupling with surface soil moisture for the semi-arid rather
798 than temperate climate (e.g. Colliander et al., 2017; Merlin et al., 2012); with evaporation being
799 the primary control on soil wetness in semi-arid conditions. Results herein have shown that
800 the R^2 of DisPATChD during semi-arid (SMAPEX-4, austral spring) and temperate climate
801 (SMAPEX-5, austral autumn) remained the same. Conversely, results from the analysis of
802 DisPATChA products agree with the results of Merlin et al. (2012), being that the R^2 of
803 DisPATChA for the semi-arid climate was significantly higher than that of DisPATChA for the
804 temperate climate. In order to avoid such a reduction of DisPATCh performance for wet soil
805 conditions, Djamaï et al. (2015) have recommended the use of a non-linear relationship between
806 soil moisture and soil evaporative efficiency instead of the linear one used herein.

807 Results also showed that the seasonal performance of DisPATCh products was similar to
808 that of passive soil moisture estimates from which the DisPATCh products originated. These
809 findings suggest that the performance of DisPATCh is heavily influenced by the performance of
810 the original passive soil moisture estimates. Therefore, the uncertainty of the original passive
811 soil moisture products is dictating the accuracy of DisPATCh. These findings are not consistent
812 with findings from Merlin et al. (2012) and Colliander et al. (2017), that proposed the coupling
813 between soil moisture and evaporative efficiency as the main factor controlling the accuracy of
814 DisPATCh products. Improvement of the accuracy of passive coarse soil moisture products is
815 therefore another requirement for improvement of DisPATCh products.

816 Based on the spatial analysis of seasonal performance, products at 1 km had similar per-
817 formance for SMAPEX-4 and SMAPEX-5 regardless of season. These results are contrasted
818 against those obtained from spatial analysis of products at 9 km. In general, products at 9
819 km had slightly better performance during SMAPEX-4 than SMAPEX-5. The stark contrast of
820 the performance of downscaled products during SMAPEX-4 and SMAPEX-5, was specifically
821 introduced for SMAP SFIM products. Reduced sensitivity of high frequency radiometer obser-

822 vations to soil moisture dynamics under increased vegetation cover and rainfall events during
823 SMAPEx-5 could be the key factor in accuracy reduction of SMAP SFIM in temperate climate.

824 **7 Conclusion**

825 This paper has presented the first analysis of the alternative downscaled soil moisture products
826 currently available against a common reference data set, to overview their applicability for the
827 applications requiring soil moisture products at resolutions higher than 10 km. While cloudy
828 skies limit the application of optical-based downscaled products, the SMAP and SMOS VTCI
829 as optical-based products had the highest level of temporal agreement with OzNet and airborne
830 PLMR soil moisture, respectively. However, they could not meet the temporal requirements
831 for applications. The use of geostationary based optical sensors which collect data at about
832 30 minute time intervals may help to overcome this shortcoming by increasing the chance of
833 capturing cloud-free observations.

834 The oversampling-based soil moisture products (SMAP EnhancedA and SMAP EnhancedD)
835 best captured the temporal and spatial variability of soil moisture overall, though the SMAP
836 MOEA and A/P had a better temporal agreement with PLMR during the short SMAPEx-4
837 period. The SMAP Enhanced products not only surpassed the other downscaled products in
838 terms of performance and accuracy, but also in terms of availability under all-weather conditions
839 and improvement of soil moisture retrieval over coarse passive microwave retrievals. Further-
840 more, the interpolation technique used for the Enhanced soil moisture production does not
841 require any concurrent data from other satellites. However, the spatial resolution of the SMAP
842 Enhanced products does not meet the requirements for application to agriculture and water
843 resources management, which need a resolution of at least 1 km.

844 The difference between temporal analysis of products against *in situ* and airborne soil mois-
845 ture reference data sets also pointed to the fact that relying on *in situ* measurement alone is
846 not appropriate for validation of soil moisture maps; basically *in situ* measurements that are

847 site specific and sparsely distributed ignored the short scale spatial variation of soil moisture.
848 Furthermore, the difference between temporal and spatial analysis of products against the air-
849 borne PLMR soil moisture maps suggests that dependence on temporal analysis is not ideal for
850 assessing the performance of spatial variation in soil moisture products. Based on the purpose of
851 the soil moisture application, spatial analysis should be conducted to quantify the performance
852 of the soil moisture products in capturing the variability of soil moisture in space.

8 Acknowledgements

This research was made possible through the financial support from an ARC Discovery Project (MoistureMonitor, DP140100572) and Infrastructure grant (LE0453434). Monash University is also acknowledged for its contribution towards a postgraduate scholarship for Sabah Sabaghy to pursue her PhD. Jian Peng was supported by the ESA SEOM project “Exploitation of S-1 for Surface Soil Moisture Retrieval at High Resolution” under Contract 4000118762/16/I-NB.

Appendix A

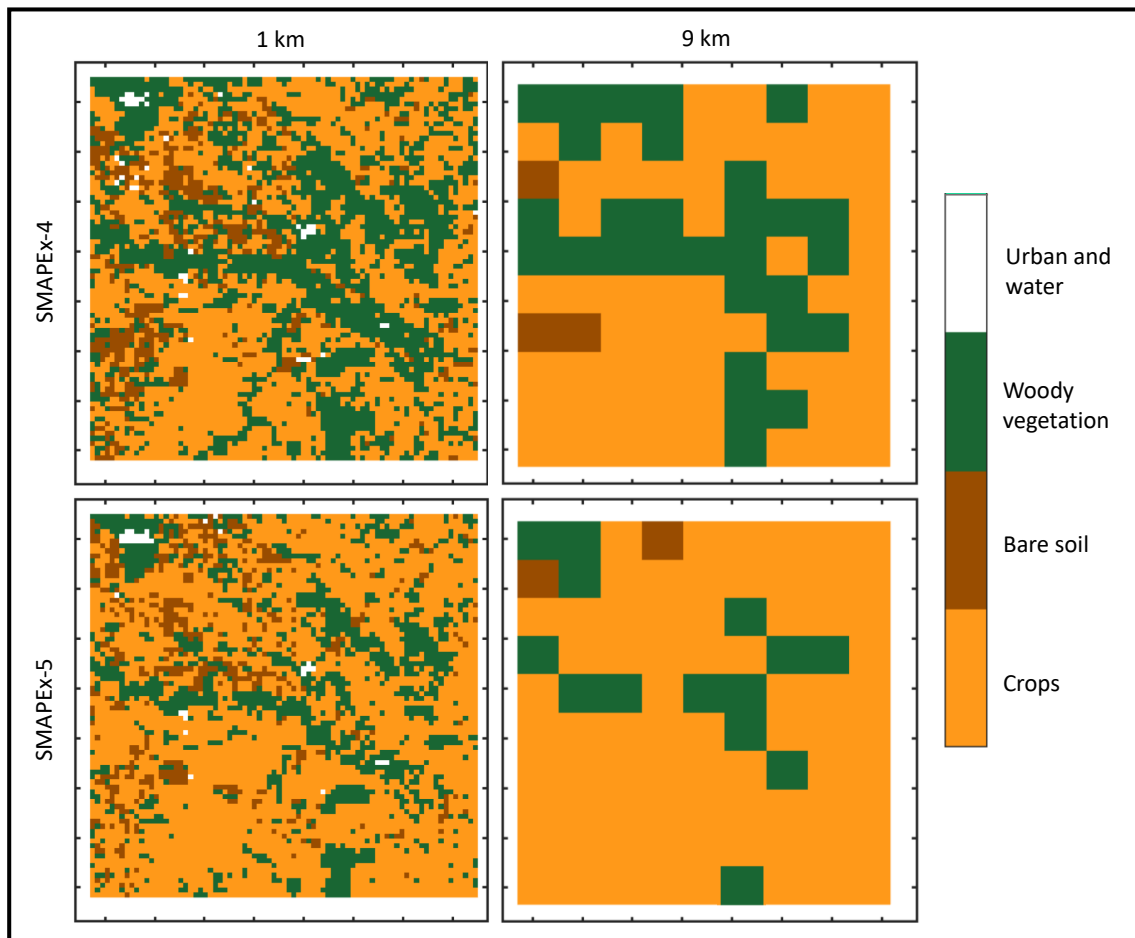


Figure A1: Land cover maps showing dominant vegetation cover at 1 and 9 km spatial resolution the same as that of downscaled soil moisture maps.

Table A1: Summary table on the relative accuracy [-] of soil moisture downscaling products at 1 km derived from their temporal analysis against OzNet *in situ* and airborne PLMR soil moisture estimates.

Downscaling Technique	Downscaled Product	Against OzNet				Against airborne PLMR (SMAPEx-4 and -5)				Against airborne PLMR (SMAPEx-4)				Against airborne PLMR (SMAPEx-5)			
		Bias	RMSD	ubRMSD	[-]	Bias	RMSD	ubRMSD	[-]	Bias	RMSD	ubRMSD	[-]	Bias	RMSD	ubRMSD	[-]
Optical-based	SMOS DisPATCHA	0.113	0.415	0.390	[-]	-0.204	0.633	0.510	[-]	-0.273	0.743	0.587	[-]	-0.083	0.401	0.170	[-]
	SMOS DisPATCHD	0.060	0.527	0.516	[-]	-0.099	0.538	0.451	[-]	-0.160	0.604	0.468	[-]	-0.134	0.488	0.329	[-]
	SMAP VTCI	0.080	0.387	0.305	[-]	-0.294	0.731	0.604	[-]	-	-	-	[-]	-0.189	0.488	0.303	[-]
	SMOS VTCI	0.005	0.540	0.494	[-]	-0.203	0.493	0.341	[-]	-	-	-	[-]	-0.421	0.519	0.230	[-]
Uniform field	SMAP PassiveA	0.110	0.395	0.363	[-]	-0.300	0.691	0.588	[-]	-0.318	0.648	0.549	[-]	-0.272	0.482	0.271	[-]
	SMAP PassiveD	0.244	0.410	0.321	[-]	-0.222	0.594	0.496	[-]	-0.148	0.394	0.292	[-]	-0.233	0.486	0.282	[-]
	SMOS PassiveA	0.141	0.336	0.314	[-]	-0.231	0.675	0.598	[-]	-0.189	0.643	0.567	[-]	-0.246	0.510	0.330	[-]
	SMOS PassiveD	0.180	0.566	0.507	[-]	-0.240	0.648	0.563	[-]	-0.099	0.481	0.379	[-]	-0.297	0.548	0.381	[-]

Table A2: As for Table A1 but for products at 9 km.

Downscaling Technique	Downscaled Product	Against OzNet				Against airborne PLMR (SMAPEx-4 and -5)				Against airborne PLMR (SMAPEx-4)				Against airborne PLMR (SMAPEx-5)			
		Bias	RMSD	ubRMSD	ubRMSD	Bias	RMSD	ubRMSD	ubRMSD	Bias	RMSD	ubRMSD	ubRMSD	Bias	RMSD	ubRMSD	ubRMSD
		[-]	[-]	[-]	[-]	[-]	[-]	[-]	[-]	[-]	[-]	[-]	[-]	[-]	[-]	[-]	[-]
Radar-based	SMAP MOEA	0.311	0.492	0.381	0.330	0.271	0.271	0.330	0.271	-0.111	0.330	0.271	-0.111	0.330	0.271	-	-
	SMAP A/P	0.404	0.770	0.646	0.488	0.341	0.341	0.488	0.341	-0.242	0.488	0.341	-0.242	0.488	0.341	-	-
Optical-based	SMOS DisPATCHA	-0.072	0.293	0.284	0.612	0.558	0.558	0.612	0.558	-0.241	0.612	0.558	-0.367	0.724	0.627	-0.148	0.336
	SMOS DisPATCHD	-0.085	0.433	0.424	0.543	0.487	0.487	0.543	0.487	-0.195	0.543	0.428	-0.169	0.531	0.428	-0.216	0.412
	SMAP VTCl	-0.148	0.241	0.191	0.654	0.568	0.568	0.654	0.568	-0.335	0.654	-	-	-	-	-0.266	0.424
	SMOS VTCl	-0.145	0.459	0.439	0.327	0.222	0.222	0.327	0.222	-0.238	0.327	-	-	-	-	-0.423	0.465
Radiometer-based	SMAP SFIM	0.209	0.372	0.311	0.486	0.432	0.432	0.486	0.432	-0.178	0.486	0.288	-0.043	0.358	0.288	-0.209	0.378
Oversampling-based	SMAP EnhancedA	0.020	0.295	0.294	0.537	0.465	0.465	0.537	0.465	-0.254	0.537	0.288	-0.098	0.288	0.223	-0.294	0.376
	SMAP EnhancedD	0.093	0.289	0.274	0.494	0.433	0.433	0.494	0.433	-0.233	0.494	0.274	-0.181	0.324	0.274	-0.264	0.379
	SMAP PassiveA	0.070	0.331	0.315	0.611	0.516	0.516	0.611	0.516	-0.322	0.611	0.647	-0.356	0.647	0.546	-0.337	0.405
Uniform field	SMAP PassiveD	0.177	0.322	0.275	0.505	0.423	0.423	0.505	0.423	-0.249	0.505	0.326	-0.183	0.326	0.252	-0.301	0.395
	SMOS PassiveA	0.068	0.269	0.260	0.594	0.534	0.534	0.594	0.534	-0.240	0.594	0.587	-0.196	0.587	0.551	-0.251	0.422
	SMOS PassiveD	0.102	0.477	0.466	0.546	0.513	0.513	0.546	0.513	-0.250	0.546	0.395	-0.101	0.395	0.361	-0.301	0.456

Table A3: Summary table on the relative accuracy [-] of soil moisture downscaling products at 1 km derived from their spatial analysis against airborne PLMR soil moisture maps.

Downscaling Technique	Downscaled Product	Against airborne PLMR (SMAPE _{x-4} and -5)				Against airborne PLMR (SMAPE _{x-4})				Against airborne PLMR (SMAPE _{x-5})			
		Bias	RMSD	ubRMSD	[-]	Bias	RMSD	ubRMSD	[-]	Bias	RMSD	ubRMSD	[-]
Optical-based	SMOS DisPATChA	0.009	0.643	0.537	0.537	-0.085	0.833	0.548	0.548	-0.077	0.524	0.520	
	SMOS DisPATChD	-0.082	0.579	0.544	0.544	-0.082	0.680	0.561	0.561	-0.216	0.584	0.501	
	SMAP VTCl	-0.127	0.520	0.446	0.446	-	-	-	-	-0.132	0.554	0.484	
	SMOS VTCl	-0.266	0.572	0.495	0.495	-	-	-	-	-0.421	0.645	0.495	
Uniform field	SMAP PassiveA	-0.068	0.522	0.465	0.465	-0.086	0.479	0.451	0.451	-0.231	0.559	0.517	
	SMAP PassiveD	-0.128	0.499	0.455	0.455	-0.181	0.456	0.422	0.422	-0.200	0.549	0.519	
	SMOS PassiveA	0.007	0.512	0.469	0.469	0.121	0.476	0.461	0.461	-0.175	0.547	0.527	
	SMOS PassiveD	-0.180	0.545	0.501	0.501	-0.122	0.540	0.438	0.438	-0.393	0.615	0.533	

Table A4: As for Table A3 but for products at 9 km.

Downscaling Technique	Downscaled Product	Against airborne PLMR (SMAPE _{x-4} and -5)				Against airborne PLMR (SMAPE _{x-4})				Against airborne PLMR (SMAPE _{x-5})			
		Bias	RMSD	ubRMSD	[-]	Bias	RMSD	ubRMSD	[-]	Bias	RMSD	ubRMSD	[-]
Radar-based	SMAP MOEA	-0.090	0.351	0.273	0.273	-0.090	0.351	0.273	0.273	-	-	-	-
	SMAP A/P	-0.087	0.525	0.509	0.509	-0.087	0.525	0.509	0.509	-	-	-	-
	SMOS DisPATCHA	-0.042	0.447	0.327	0.327	-0.086	0.544	0.393	0.393	-0.138	0.347	0.306	0.306
Optical-based	SMOS DisPATCHD	-0.177	0.387	0.327	0.327	-0.062	0.387	0.344	0.344	-0.367	0.508	0.281	0.281
	SMAP VTCl	-0.128	0.317	0.265	0.265	-	-	-	-	-0.140	0.402	0.244	0.244
	SMOS VTCl	-0.271	0.377	0.261	0.261	-	-	-	-	-0.447	0.524	0.265	0.265
Radiometer-based	SMAP SFIM	0.039	0.373	0.238	0.238	-0.007	0.370	0.202	0.202	-0.238	0.344	0.231	0.231
Oversampling-based	SMAP EnhancedA	-0.082	0.274	0.222	0.222	-0.074	0.225	0.213	0.213	-0.222	0.354	0.242	0.242
	SMAP EnhancedD	-0.103	0.290	0.224	0.224	-0.110	0.286	0.189	0.189	-0.222	0.354	0.242	0.242
	SMAP PassiveA	-0.086	0.312	0.267	0.267	-0.091	0.261	0.245	0.245	-0.259	0.362	0.262	0.262
Uniform field	SMAP PassiveD	-0.114	0.313	0.250	0.250	-0.158	0.297	0.233	0.233	-0.236	0.369	0.262	0.262
	SMOS PassiveA	0.020	0.309	0.233	0.233	0.158	0.307	0.230	0.230	-0.178	0.368	0.248	0.248
	SMOS PassiveD	-0.124	0.389	0.230	0.230	-0.089	0.270	0.230	0.230	-0.407	0.497	0.248	0.248

References

- R. Akbar and M. Moghaddam. A combined active-passive soil moisture estimation algorithm with adaptive regularization in support of SMAP. *IEEE Transactions on Geoscience and Remote Sensing*, 53(6):3312–3324, 2015.
- R. Akbar, S. Chan, N. Das, S. Kim, D. Entekhabi, and M. Moghaddam. A multi-objective optimization approach to combined radar-radiometer soil moisture estimation. In *IEEE International Geoscience and Remote Sensing Symposium (IGARSS)*, pages 3074–3077, July 2016.
- A. Al-Yaari, J.-P. Wigneron, W. Dorigo, A. Colliander, T. Pellarin, S. Hahn, A. Mialon, P. Richaume, R. Fernandez-Moran, L. Fan, Y. Kerr, and G. D. Lannoy. Assessment and inter-comparison of recently developed/reprocessed microwave satellite soil moisture products using ISMN ground-based measurements. *Remote Sensing of Environment*, 224:289 – 303, 2019.
- M. C. Anderson, J. M. Norman, J. R. Mecikalski, J. A. Otkin, and W. P. Kustas. A climatological study of evapotranspiration and moisture stress across the continental united states based on thermal remote sensing: 1. model formulation. *Journal of Geophysical Research: Atmospheres*, 112(D10), 2007.
- G. Backus and F. Gilbert. Uniqueness in the inversion of inaccurate gross earth data. *Philosophical Transactions of the Royal Society of London A: Mathematical, Physical and Engineering Sciences*, 266(1173):123–192, 1970.
- G. E. Backus and J. Gilbert. Numerical applications of a formalism for geophysical inverse problems. *Geophysical Journal International*, 13(1-3):247–276, 1967.
- R. Bindlish, T. Jackson, M. Cosh, S. Ruijing, S. Yueh, and S. Dinardo. Combined passive and

- active soil moisture observations during classic. In *IEEE International Geoscience and Remote Sensing Symposium (IGARSS)*, volume 2, pages II-237–II-240, 2008.
- J. D. Bolten, W. T. Crow, X. Zhan, T. J. Jackson, and C. A. Reynolds. Evaluating the utility of remotely sensed soil moisture retrievals for operational agricultural drought monitoring. *IEEE Journal of Selected Topics in Applied Earth Observations and Remote Sensing*, 3(1): 57–66, 2010.
- Bureau of Meteorology. Climate statistics for Australian locations. Australian Government, 2018. URL <http://www.bom.gov.au/climate/data/>.
- T. N. Carlson, R. R. Gillies, and E. M. Perry. A method to make use of thermal infrared temperature and ndvi measurements to infer surface soil water content and fractional vegetation cover. *Remote Sensing Reviews*, 9(1-2):161–173, 1994.
- S. Chan, R. Bindlish, P. O’Neill, T. Jackson, E. Njoku, S. Dunbar, J. Chaubell, J. Piepmeier, S. Yueh, D. Entekhabi, A. Colliander, F. Chen, M. Cosh, T. Caldwell, J. Walker, A. Berg, H. McNairn, M. Thibeault, J. Martínez-Fernández, F. Uldall, M. Seyfried, D. Bosch, P. Starks, C. H. Collins, J. Prueger, R. van der Velde, J. Asanuma, M. Palecki, E. Small, M. Zreda, J. Calvet, W. Crow, and Y. Kerr. Development and assessment of the SMAP enhanced passive soil moisture product. *Remote Sensing of Environment*, 204:931–941, 2018.
- J. Chaubell. SMAP algorithm theoretical basis document: SMAP L1B enhancement radiometer brightness temperature data product. Jet Propulsion Laboratory, 2016.
- N. S. Chauhan. Soil moisture estimation under a vegetation cover: Combined active passive microwave remote sensing approach. *International Journal of Remote Sensing*, 18(5):1079–1097, 1997.
- F. Chen, W. T. Crow, R. Bindlish, A. Colliander, M. S. Burgin, J. Asanuma, and K. Aida.

- Global-scale evaluation of smap, smos and ascat soil moisture products using triple collocation. *Remote Sensing of Environment*, 214:1 – 13, 2018.
- A. Colliander, J. B. Fisher, G. Halverson, O. Merlin, S. Misra, R. Bindlish, T. J. Jackson, and S. Yueh. Spatial downscaling of SMAP soil moisture using MODIS land surface temperature and NDVI during SMAPVEX15. *IEEE Geoscience and Remote Sensing Letters*, 14(11): 2107–2111, 2017.
- C. Corradini. Soil moisture in the development of hydrological processes and its determination at different spatial scales. *Journal of Hydrology*, 516:1 – 5, 2014.
- R. Crago and W. Brutsaert. Daytime evaporation and the self-preservation of the evaporative fraction and the bowen ratio. *Journal of Hydrology*, 178(1–4):241–255, 1996.
- N. N. Das, D. Entekhabi, and E. G. Njoku. An algorithm for merging SMAP radiometer and radar data for high-resolution soil-moisture retrieval. *IEEE Transactions on Geoscience and Remote Sensing*, 49(5):1504–1512, 2011.
- N. N. Das, D. Entekhabi, E. G. Njoku, J. J. C. Shi, J. T. Johnson, and A. Colliander. Tests of the SMAP combined radar and radiometer algorithm using airborne field campaign observations and simulated data. *IEEE Transactions on Geoscience and Remote Sensing*, 52(4):2018–2028, 2014.
- N. Djamaï, R. Magagi, K. Goita, O. Merlin, Y. Kerr, and A. Walker. Disaggregation of SMOS soil moisture over the Canadian Prairies. *Remote Sensing of Environment*, 170:255–268, 2015.
- D. Entekhabi, T. J. Jackson, E. Njoku, P. O’Neill, and J. Entin. Soil Moisture Active/Passive (SMAP) Mission concept. volume 7085, 2008.
- D. Entekhabi, E. G. Njoku, P. E. O’Neill, K. H. Kellogg, W. T. Crow, W. N. Edelstein, J. K. Entin, S. D. Goodman, T. J. Jackson, J. Johnson, J. Kimball, J. R. Piepmeier, R. D. Koster, N. Martin, K. C. McDonald, M. Moghaddam, S. Moran, R. Reichle, J. C. Shi, M. W. Spencer,

- S. W. Thurman, T. Leung, and J. Van Zyl. The Soil Moisture Active Passive (SMAP) Mission. *Proceedings of the IEEE*, 98(5):704–716, 2010.
- B. Fang, V. Lakshmi, R. Bindlish, T. J. Jackson, M. Cosh, and J. Basara. Passive microwave soil moisture downscaling using vegetation index and skin surface temperature. *Vadose Zone Journal*, 12(3), 2013.
- Y. Gao, J. P. Walker, M. Allahmoradi, A. Monerri, R. Dongryeol, and T. J. Jackson. Optical sensing of vegetation water content: A synthesis study. *IEEE Journal of Selected Topics in Applied Earth Observations and Remote Sensing*, 8(4):1456–1464, 2015.
- A. I. Gevaert, R. M. Parinussa, L. J. Renzullo, A. I. J. M. van Dijk, and R. A. M. de Jeu. Spatio-temporal evaluation of resolution enhancement for passive microwave soil moisture and vegetation optical depth. *International Journal of Applied Earth Observation and Geoinformation*, 2015.
- R. R. Gillies and T. N. Carlson. Thermal remote sensing of surface soil water content with partial vegetation cover for incorporation into climate models. *Journal of Applied Meteorology*, 34(4):745–756, 1995.
- J. P. Grant, K. Saleh-Contell, J. P. Wigneron, M. Guglielmetti, Y. H. Kerr, M. Schwank, N. Skou, and A. A. V. de Griend. Calibration of the L-MEB model over a coniferous and a deciduous forest. *IEEE Transactions on Geoscience and Remote Sensing*, 46(3):808–818, 2008.
- T. J. Jackson. Iii. measuring surface soil moisture using passive microwave remote sensing. *Hydrological Processes*, 7(2):139–152, 1993.
- E. Jacqueline, Y. Kerr, A. A. Bitar, F. Cabot, A. Mialon, P. Richaume, A. Quesney, and L. Berthon. CATDS SMOS L3 soil moisture retrieval processor, algorithm theoretical baseline document (ATBD), 2013.

- Y. Kerr, J. Wigneron, A. Al Bitar, A. Mialon, and P. Srivastava. Soil moisture from space: Techniques and limitations. *Satellite Soil Moisture Retrieval: Techniques and Applications*, page 1, 2016.
- R. D. Koster, P. A. Dirmeyer, Z. Guo, G. Bonan, E. Chan, P. Cox, C. T. Gordon, S. Kanae, E. Kowalczyk, D. Lawrence, P. Liu, C.-H. Lu, S. Malyshev, B. McAvaney, K. Mitchell, D. Mocko, T. Oki, K. Oleson, A. Pitman, Y. C. Sud, C. M. Taylor, D. Verseghy, R. Vasic, Y. Xue, and T. Yamada. Regions of strong coupling between soil moisture and precipitation. *Science*, 305(5687):1138–1140, 2004.
- R. D. Koster, S. P., P. M., T. J. Yamada, G. Balsamo, A. A. Berg, M. Boissierie, P. A. Dirmeyer, F. Doblas-Reyes, G. Drewitt, C. T. Gordon, Z. Guo, J. . Jeong, D. M. Lawrence, W. . Lee, Z. Li, L. Luo, S. Malyshev, W. J. Merryfield, S. I. Seneviratne, T. Stanelle, B. J., J. M. v. d. H., F. Vitart, and E. F. Wood. Contribution of land surface initialization to subseasonal forecast skill: First results from a multi-model experiment. *Geophysical Research Letters*, 37(2), 2010.
- C. Li, H. Lu, K. Yang, M. Han, J. S. Wright, Y. Chen, L. Yu, S. Xu, X. Huang, and W. Gong. The evaluation of SMAP enhanced soil moisture products using high-resolution model simulations and in-situ observations on the tibetan plateau. *Remote Sensing*, 10(4), 2018. ISSN 2072-4292.
- J. G. Liu. Smoothing filter-based intensity modulation: A spectral preserve image fusion technique for improving spatial details. *International Journal of Remote Sensing*, 21(18):3461–3472, 2000.
- D. Long, L. Bai, L. Yan, C. Zhang, W. Yang, H. Lei, J. Quan, X. Meng, and C. Shi. Generation of spatially complete and daily continuous surface soil moisture of high spatial resolution. *Remote Sensing of Environment*, 233:111364, 2019. ISSN 0034-4257. doi: <https://doi.org/>

10.1016/j.rse.2019.111364. URL <http://www.sciencedirect.com/science/article/pii/S0034425719303839>.

D. G. Long. Reconstruction and resolution enhancement techniques for microwave sensors. 2003.

D. G. Long and D. L. Daum. Spatial resolution enhancement of SSM/I data. *IEEE Transactions on Geoscience and Remote Sensing*, 36(2):407–417, 1998.

O. Merlin, A. Chehbouni, Y. H. Kerr, and D. C. Goodrich. A downscaling method for distributing surface soil moisture within a microwave pixel: Application to the monsoon '90 data. *Remote Sensing of Environment*, 101(3):379–389, 2006.

O. Merlin, A. Chehbouni, J. P. Walker, R. Panciera, and Y. H. Kerr. A simple method to disaggregate passive microwave-based soil moisture. *IEEE Transactions on Geoscience and Remote Sensing*, 46(3):786–796, 2008a.

O. Merlin, J. P. Walker, A. Chehbouni, and Y. Kerr. Towards deterministic downscaling of SMOS soil moisture using MODIS derived soil evaporative efficiency. *Remote Sensing of Environment*, 112(10):3935–3946, 2008b.

O. Merlin, C. Rudiger, A. Al Bitar, P. Richaume, J. P. Walker, and Y. H. Kerr. Disaggregation of SMOS soil moisture in southeastern Australia. *IEEE Transactions on Geoscience and Remote Sensing*, 50(5):1556–1571, 2012.

O. Merlin, M. J. Escorihuela, M. A. Mayoral, O. Hagolle, A. Al Bitar, and Y. Kerr. Self-calibrated evaporation-based disaggregation of SMOS soil moisture: An evaluation study at 3km and 100m resolution in Catalunya, Spain. *Remote Sensing of Environment*, 130(0):25–38, 2013.

O. Merlin, Y. Malbêteau, Y. Notfi, S. Bacon, S. Khabba, and L. Jarlan. Performance metrics for

- soil moisture downscaling methods: Application to dispatch data in central morocco. *Remote Sensing*, 7(4):3783–3807, 2015.
- V. Mishra, W. L. Ellenburg, R. E. Griffin, J. R. Mecikalski, J. F. Cruise, C. R. Hain, and M. C. Anderson. An initial assessment of a SMAP soil moisture disaggregation scheme using TIR surface evaporation data over the continental United States. *International Journal of Applied Earth Observation and Geoinformation*, 68:92 – 104, 2018. ISSN 0303-2434.
- B. Molero, O. Merlin, Y. Malbêteau, A. Al Bitar, F. Cabot, V. Stefan, Y. Kerr, S. Bacon, M. H. Cosh, R. Bindlish, and T. J. Jackson. SMOS disaggregated soil moisture product at 1 km resolution: Processor overview and first validation results. *Remote Sensing of Environment*, 180:361–376, 2016.
- M. S. Moran, T. R. Clarke, Y. Inoue, and A. Vidal. Estimating crop water deficit using the relation between surface-air temperature and spectral vegetation index. *Remote Sensing of Environment*, 49(3):246–263, 1994.
- P. O’Neill, D. Entekhabi, E. Njoku, and K. Kellogg. The NASA Soil Moisture Active Passive (SMAP) mission: Overview. In *IEEE International Geoscience and Remote Sensing Symposium (IGARSS)*, pages 3236–3239, 2010.
- M. Owe, R. de Jeu, and J. Walker. A methodology for surface soil moisture and vegetation optical depth retrieval using the microwave polarization difference index. 39:1643 – 1654, 09 2001.
- M. Owe, R. de Jeu, and T. Holmes. Multisensor historical climatology of satellite-derived global land surface moisture. *Journal of Geophysical Research: Earth Surface*, 113(F1), 2008.
- R. Panciera, J. P. Walker, J. D. Kalma, E. J. Kim, J. M. Hacker, O. Merlin, M. Berger, and N. Skou. The NAFE’05/CoSMOS data set: Toward SMOS soil moisture retrieval, downscal-

- ing, and assimilation. *IEEE Transactions on Geoscience and Remote Sensing*, 46(3):736–745, 2008.
- R. Panciera, J. P. Walker, J. D. Kalma, E. J. Kim, K. Saleh, and J.-P. Wigneron. Evaluation of the SMOS L-MEB passive microwave soil moisture retrieval algorithm. *Remote Sensing of Environment*, 113(2):435–444, 2009.
- J. Peng, J. Niesel, and A. Loew. Evaluation of soil moisture downscaling using a simple thermal-based proxy – the REMEDHUS network (Spain) example. *Hydrology and Earth System Sciences*, 19(12):4765–4782, 2015.
- J. Peng, A. Loew, Z. Shiqiang, W. Jie, and J. Niesel. Spatial downscaling of satellite soil moisture data using a vegetation temperature condition index. *IEEE Transactions on Geoscience and Remote Sensing*, 54(1):558–566, 2016.
- J. Peng, A. Loew, O. Merlin, and N. E. C. Verhoest. A review of spatial downscaling of satellite remotely sensed soil moisture. *Reviews of Geophysics*, 2017.
- G. P. Petropoulos, G. Ireland, and B. Barrett. Surface soil moisture retrievals from remote sensing: Current status, products & future trends. *Physics and Chemistry of the Earth, Parts A/B/C*, (0), 2015.
- M. Piles, D. Entekhabi, and A. Camps. A change detection algorithm for retrieving high-resolution soil moisture from SMAP radar and radiometer observations. *IEEE Transactions on Geoscience and Remote Sensing*, 47(12):4125–4131, 2009.
- M. Piles, A. Camps, M. Vall-llossera, I. Corbella, R. Panciera, C. Rudiger, Y. H. Kerr, and J. Walker. Downscaling SMOS-derived soil moisture using MODIS visible/infrared data. *IEEE Transactions on Geoscience and Remote Sensing*, 49(9):3156–3166, 2011.
- M. Piles, M. Vall-llossera, L. Laguna, and A. Camps. A downscaling approach to combine SMOS multi-angular and full-polarimetric observations with MODIS VIS/IR data into high resolu-

- tion soil moisture maps. In *IEEE International Geoscience and Remote Sensing Symposium (IGARSS)*, pages 1247–1250, 22-27 July 2012. ISBN 2153-6996.
- M. Piles, M. Vall-llossera, A. Camps, N. Sánchez, J. Martínez-Fernández, J. Martínez, V. González-Gambau, and R. Riera. On the synergy of SMOS and Terra/Aqua MODIS: High resolution soil moisture maps in near real-time. In *IEEE International Geoscience and Remote Sensing Symposium (IGARSS)*, pages 3423–3426, 21-26 July 2013. ISBN 2153-6996.
- M. Piles, G. P. Petropoulos, N. Sánchez, n. González-Zamora, and G. Ireland. Towards improved spatio-temporal resolution soil moisture retrievals from the synergy of SMOS and MSG SEVIRI spaceborne observations. *Remote Sensing of Environment*, 180:403–417, 2016.
- G. A. Poe. Optimum interpolation of imaging microwave radiometer data. *IEEE Transactions on geoscience and remote sensing*, 28(5):800–810, 1990.
- J. W. Rouse, R. Haas, J. Schell, and D. Deering. Monitoring vegetation systems in the great plains with erts. 1974.
- S. Sabaghy, J. P. Walker, L. J. Renzullo, and T. J. Jackson. Spatially enhanced passive microwave derived soil moisture: Capabilities and opportunities. *Remote Sensing of Environment*, 209:551 – 580, 2018.
- E. Santi. An application of the SFIM technique to enhance the spatial resolution of spaceborne microwave radiometers. *International Journal of Remote Sensing*, 31(9):2419–2428, 2010.
- S. I. Seneviratne, T. Corti, E. L. Davin, M. Hirschi, E. B. Jaeger, I. Lehner, B. Orlowsky, and A. J. Teuling. Investigating soil moisture–climate interactions in a changing climate: A review. *Earth-Science Reviews*, 99(3–4):125–161, 2010.
- A. B. Smith, J. P. Walker, A. W. Western, R. I. Young, K. M. Ellett, R. C. Pipunic, R. B. Grayson, L. Siritwidena, F. H. S. Chiew, and H. Richter. The Murrumbidgee soil moisture monitoring network data set. *Water Resources Research*, 48(W07701):6pp., 2012.

- R. van der Velde, M. S. Salama, M. D. van Helvoirt, Z. Su, and Y. Ma. Decomposition of uncertainties between coarse MM5–Noah-simulated and fine ASAR-retrieved soil moisture over Central Tibet. *Journal of Hydrometeorology*, 13(6):1925–1938, 2012.
- P.-X. Wang, X.-W. Li, J.-Y. Gong, and C. Song. Vegetation temperature condition index and its application for drought monitoring. In *IEEE International Geoscience and Remote Sensing Symposium (IGARSS)*, volume 1, pages 141–143, 2001.
- J. P. Wigneron, Y. Kerr, P. Waldteufel, K. Saleh, M. J. Escorihuela, P. Richaume, P. Ferrazoli, P. de Rosnay, R. Gurney, J. C. Calvet, J. P. Grant, M. Guglielmetti, B. Hornbuckle, C. Mätzler, T. Pellarin, and M. Schwank. L-band microwave emission of the biosphere (L-MEB) model: Description and calibration against experimental data sets over crop fields. *Remote Sensing of Environment*, 107(4):639–655, 2007.
- X. Wu, J. P. Walker, N. N. Das, R. Panciera, and C. Rüdiger. Evaluation of the SMAP brightness temperature downscaling algorithm using active–passive microwave observations. *Remote Sensing of Environment*, 155(0):210–221, 2014.
- X. Wu, J. P. Walker, C. Rudiger, R. Panciera, and D. A. Gray. Simulation of the SMAP data stream from SMAPEX field campaigns in Australia. *IEEE Transactions on Geoscience and Remote Sensing*, 53(4):1921–1934, 2015.
- X. Wu, J. P. Walker, C. Rüdiger, R. Panciera, and Y. Gao. Intercomparison of alternate soil moisture downscaling algorithms using active-passive microwave observations. *IEEE Geoscience and Remote Sensing Letters*, PP(99):1–5, 2016.
- N. Ye, J. P. Walker, and C. Rüdiger. A cumulative distribution function method for normalizing variable-angle microwave observations. *IEEE Transactions on Geoscience and Remote Sensing*, 53(7):3906–3916, 2015.
- N. Ye, J. P. Walker, X. Wu, R. d. Jeu, D. Entekhabi, Y. Gao, T. J. Jackson, F. Jonard, E. Kim,

- O. Merlin, V. Pauwels, L. Renzullo, C. Rüdiger, S. Sabaghy, C. v. H. e, S. H. Yueh, and L. Z. a. The soil moisture active passive experiments: Towards calibration and validation of the SMAP mission. *IEEE Transactions on Geoscience and Remote Sensing*, in review.
- M. S. Yee, J. P. Walker, A. Monerris, C. Rüdiger, and T. J. Jackson. On the identification of representative in situ soil moisture monitoring stations for the validation of SMAP soil moisture products in Australia. *Journal of Hydrology*, 537:367 – 381, 2016.
- X. Zhan, P. R. Houser, J. P. Walker, and W. T. Crow. A method for retrieving high-resolution surface soil moisture from hydros l-band radiometer and radar observations. *IEEE Transactions on Geoscience and Remote Sensing*, 44(6):1534–1544, 2006.
- W. Zhao and A. Li. A downscaling method for improving the spatial resolution of AMSR-E derived soil moisture product based on MSG-SEVIRI data. *Remote Sensing*, 5(12):6790, 2013.